646 *Macromolecules* **1996,** *29,* 646−660

Fluorophobic Effect in the Self-Assembly of Polymers and Model Compounds Containing Tapered Groups into Supramolecular Columns

G. Johansson and V. Percec*

The W. M. Keck Laboratories for Organic Synthesis, Department of Macromolecular Science, Case Western Reserve University, Cleveland, Ohio 44106-7202

G. Ungar and J. P. Zhou

Department of Engineering Materials and Centre for Molecular Materials, University of Sheffield, Sheffield S1 4DU, U.K.

Received August 8, 1995; Revised Manuscript Received October 27, 1995[⊗]

ABSTRACT: The synthesis and characterization of the tapered building blocks 3,4,5-tris(1*H*,1*H*,2*H*,2*H*,3*H*,3*H*,4*H*,4*H*,5*H*,5*H*,6*H*,6*H*,7*H*,7*H*,8*H*,8*H*-perfluorododecan-1-yloxy)benzoic acid (**11-8/4**), 3,4,5-tris(1*H*,1*H*,2*H*,2*H*,3*H*,3*H*,4*H*,4*H*,5*H*,5*H*,6*H*,6*H*-perfluorododecan-1-yloxy)benzoic acid (**11-6/6**), 3,4,5-tris(1*H*,1*H*,2*H*,2*H*,3*H*,3*H*,4*H*,4*H*-perfluorododecan-1-yloxy)benzoic acid (**11-4/8**), 2-{2-[2-(2-hydroxyethoxy)ethoxy]ethoxy}ethyl 3,4,5-tris(1*H*,1*H*,2*H*,2*H*,3*H*,3*H*,4*H*,4*H*,5*H*,5*H*,6*H*,6*H*,7*H*,7*H*,8*H*,8*H*-perfluorododecan-1-yloxy)benzoate (**19-8/4**), 2-{2-[2-(2-hydroxyethoxy)ethoxy]ethoxy}ethyl 3,4,5-tris(1*H*,1*H*,2*H*,2*H*,3*H*,3*H*,4*H*,4*H*,5*H*,5*H*,6*H*,6*H*-perfluorododecan-1-yloxy)benzoate (**19-6/6**), and 2-{2-[2-(2-hydroxyethoxy)ethoxy]ethoxy}ethyl 3,4,5-tris(1*H*,1*H*,2*H*,2*H*,3*H*,3*H*,4*H*,4*H*-perfluorododecan-1-yloxy)benzoate (**19-4/8**) and of the methacrylates and polymethacrylates of **19-8/4**, **19-6/6**, and **19-4/8** (i.e, **20-8/4**, **20-6/6**, **20-4/8** and respectively **21-8/4**, **21-6/6**, and **21-4/8**) are described. All tapered building blocks **11-m/n**, **19-m/n**, and the polymers **21-m/n** (where $\mathbf{m} + \mathbf{n} = 12$ and $\mathbf{m}$ = number of hydrogenated, $\mathbf{n}$ = number of perfluorinated methylenic groups of their alkyl tails) self-assemble into tubular supramolecular architectures which display an enantiotropic hexagonal columnar (Φ_h) mesophase. The self-assembling ability of model compounds and polymers was compared to that of their perhydrogenated analogues. From the perhydrogenated compounds, only the polymer **21-12/0** forms a Φ_h phase. Semifluorination of all model compounds and polymers first decreases the melting temperature of the supramolecular assembly and uncovers and/or enhances the thermal stability of the Φ_h phase ($\mathbf{n} = 4$). A further increase of **n** from 4 to 6 and respectively 8 increases both the isotropization temperature of the Φ_h phase and the melting temperature. A parallel increase of the diameter of the supramolecular columns with the increase of **n** is observed. A mechanism for this dramatic increase in the self-assembly process *via* microsegregation of the perfluorinated and perhydrogenated parts of the tapered groups due to the fluorophobic effect was proposed.

Introduction

We are concerned with the molecular design of tapered building blocks (i.e., *exo*-receptors) containing various *endo*-receptors which self-assemble into tubular supramolecular architectures which in turn are responsible for the formation of hexagonal columnar (Φ_h) liquid crystalline assemblies.[1,2,3] The *endo*-receptor of these tapered building blocks can be replaced with or be covalently bound to a suitable polymer backbone to generate polymers which by analogy with their low molar mass homologues self-assemble into tubular architectures.[1c−e,2,3] Simultaneously, we are investigating the mechanism of self-assembly of both low molar mass and polymeric structures based on tapered building blocks. In the case of polymers, most probably, the tubular structure is based on a single backbone surrounded by its own tapered side groups. By analogy with the case of the self-assembly of rod-like viruses, the random-coil conformation of the backbone should be distorted into a helical-like one.[2,3] The ability of a certain polymer backbone to distort its own conformation is determined mainly by the capability of its tapered side group to overcome the entropy loss during self-assembly. The first step of the self-assembly of low molar mass building blocks consists of the formation of a supramolecular disc-like unit. Briefly, these tapered groups play the role of the bricks in the assembly of a construction. Their shape determines the shape of the construction. At the same time, the wider and stronger they are, the more stable is the resulting construction. An additional increase of the stability of this construction is provided by using a cement. Its role in our previous investigations was played by the various *endo*-receptors which generated ionic, H-bonding, and other noncovalent interactions, and also by the polymer backbone.

The tapered building blocks employed presently in our group are based on 3,4,5-trihydroxybenzoate derivatives such as 3,4,5-tris[(4-(*n*-alkan-1-yloxy)benzyl)oxy]benzoate and 3,4,5-tris(*n*-alkan-1-yloxy)benzoate, respectively.[1] These groups represent the first generation of a monodendron which has two branching points in each repeat unit. For the same *endo*-receptor, the ability of these two classes of tapered side groups to generate a tubular supramolecular architecture is determined by the length of their *n*-alkan-1-yloxy groups.[1,2]

It is well-known that perfluorinated alkanes are more rigid and less miscible (fluorophobic effect) than the corresponding perhydrogenated alkanes.[4] As a consequence, the replacement of a perhydrogenated alkane with a perfluorinated one in the tail of a rod-like molecular liquid crystal enhances the thermal stability of the liquid crystalline phase.[5] At the same time, a suitable proportion between the perfluorinated and perhydrogenated segments within the same molecule

---

[⊗] Abstract published in *Advance ACS Abstracts,* December 15, 1995.

produces a microsegregation at the molecular level, and this process can be alone responsible for the formation of lamellar thermotropic[6,7] and lyotropic mesophases.[8]

In a previous publication from our laboratory[9] we have reported that the replacement of the outer six of the ten methylenic units of the alkyl tails of 3,4,5-tris[(4-(*n*-decan-1-yloxy)benzyl)oxy]benzoate and of 3,4,5-tris(*n*-decan-1-yloxy)benzoate, respectively, with perfluorinated methylenic groups produces a dramatic enhancement of the ability of these building blocks to self-assemble into supramolecular columnar architectures and subsequently into Φ_h mesophases. This stabilization of the Φ_h mesophase is of interest for the molecular design of supramolecular columns with various diameters and functionalities in the core of these columns, for the understanding of the self-assembly mechanism, and for the design of supramolecular objects with a perfluorinated surface. The investigation of the influence of the extent of fluorination of the alkyl tails of the tapered group on the stabilization of the Φ_h mesophase generated from them represents the first step toward the understanding of the fluorophobic effect on this self-assembly process.

The goal of this paper is to report the synthesis and characterization of the model compounds 3,4,5-tris(*n*-dodecan-1-yloxy)benzoic acid (**11-12/0**), 2-{2-[2-(2-hydroxyethoxy)ethoxy]ethoxy}ethyl 3,4,5-tris(*n*-dodecan-1-yloxy)benzoate (**19-12/0**), and poly{2-{2-[2-(2-(methacryloyloxy)ethoxy)ethoxy]ethoxy}ethyl 3,4,5-tris(*n*-dodecan-1-yloxy)benzoate} (**21-12/0**), in which 4, 6, and 8 of the outer methylene groups of the *n*-dodecan-1-yloxy tails were replaced with perfluorinated groups, i.e., **11-m/n**, **19-m/n**, and **21-m/n**, where $\mathbf{m} + \mathbf{n} = 12$, and **m** represents the number of perhydrogenated and **n** of perfluorinated methylenic groups. **11-12/0** and **19-12/0** are only crystalline, while the polymer **21-12/0** forms a supramolecular column which generates a Φ_h phase. All semifluorinated compounds **11-m/n**, **19-m/n**, and **21-m/n**, with $\mathbf{n} = 4$, 6, or 8, self-assemble into supramolecular columns which disply Φ_h phases. The influence of the extent of fluorination on the ability of these tapered groups to self-assemble into supramolecular columns, on the diameter of the supramolecular columns, and on the thermal stability of the Φ_h mesophase resulting from these columns will be discussed. These experiments provide the first series of quantitative results on the fluorophobic effect in the self-assembly of tapered groups into supramolecular columns.

Experimental Section

Materials. 1,5-Pentanediol (97%), HBr (ACS reagent, 48%), allyl bromide (99%), $CuCl_2$ (anhydrous, 97%), $LiAlH_4$ (95+%), tricaprylmethylammonium chloride (Aliquat 336), methyl 3,4,5-trihydroxybenzoate (**9**) (98%), 1,6-dibromohexane (**12**) (97%), hexamethylphosphoramide (HMPA) (99%), tributyltin hydride (n-Bu_3SnH) (97%), vinylacetic acid (**7**) (97%), $SOCl_2$ (99+%), $(C_2H_5)_3N$ (99%), 1,3-dicyclohexylcarbodiimide (DCC) (99%), and 4-(dimethylamino)pyridine (DMAP) (99%) (all from Aldrich) were used as received. 2,3-Dihydropyran (DHP) (Fluka, 97%) and palladium, 5% on carbon (Lancaster), were used as received. *p*-Toluenesulfonic acid monohydrate (*p*-TsOH), LiCl (anhydrous), and 1,1,2-trichloro-1,2,2-trifluoroethane (Freon 113) (all from Fisher Scientific) were used as received. Perfluorobutyl iodide (Aldrich, 98%), perfluorohexyl iodide (99%), and perfluorooctyl iodide (>98%) (both from Fluka) were washed with 10% $Na_2S_2O_3$ and dried over anhydrous $MgSO_4$ prior to use. 2,2′-Azobis(2-methylpropionitrile) (AIBN) (Eastman, 99%) was recrystallized from methanol. Methacryloyl chloride (Fluka, >97%) was distilled under vacuum at room temperature. Tetrahydrofuran (THF) (ACS reagent, Fisher Scientific) was refluxed over sodium ketyl and distilled freshly before use. Hexanes (ACS reagent, Fisher Scientific) used for the Pd(0) catalyzed coupling of perfluoroalkyl iodides and olefins was washed three times with concentrated H_2SO_4, three times with H_2O, and dried over anhydrous $MgSO_4$ before use. Benzene (low thiophene grade, Fisher Scientific) was washed three times with H_2SO_4 and three times with H_2O, dried over anhydrous $MgSO_4$, and further dried by refluxing over sodium ketyl, followed by fresh distillation before use. Methylene chloride (CH_2Cl_2) (Fisher) was dried by refluxing over CaH_2 and freshly distilled before use. *N*,*N*-Dimethylformamide (DMF) (Fisher, ACS reagent) was used as received. A 0.1 M Li_2CuCl_4 solution in THF was prepared by dissolving LiCl (0.42 g, 10 mmol) and $CuCl_2$ (0.67 g, 5.0 mmol) in 50 mL of anhydrous THF.[10]

Techniques. ^{1}H NMR (200 MHz), ^{19}F NMR (188 MHz), and ^{13}C NMR (50 MHz) spectra were recorded on a Varian Gemini 200 spectrometer. $CDCl_3$ was used as solvent and TMS as internal standard unless otherwise noted. Chemical shifts are reported as δ, ppm. Infrared (IR) spectra were recorded on a Perkin Elmer 1320 infrared spectrometer. The purity of products was determined by a combination of thin layer chromatography (TLC) on silica gel plates (Kodak) with fluorescent indicator and high pressure liquid chromatography (HPLC) using a Perkin-Elmer Series 10 high pressure liquid chromatograph equipped with an LC-100 column oven, Nelson Analytical 900 Series integrator data station, and two Perkin-Elmer PL gel columns of 5×10^2 and 1×10^4 Å. THF was used as solvent at the oven temperature of 40 °C unless otherwise noted. Detection was by UV absorbance at 254 nm. Weight average (M_w) and number average (M_n) molecular weights were determined with the same instrument from a calibration plot constructed from polystyrene standards. In some instances, purity was determined by gas chromatography (GC) using a Hewlett Packard 5890A gas chromatograph equipped with a Hewlett Packard 3392A integrator. A packed column consisting of 10% SP2100 on 80/100 Supelcoport stationary phase was used with a head pressure of 40−60 psi. The carrier gas was N_2.

Thermal transitions were measured on a Perkin Elmer DSC-7 differential scanning calorimeter (DSC). In all cases, the heating and cooling rates were 10 °C min^{-1} unless otherwise noted. First order transition temperatures were reported as the maxima and minima of their endothermic and exothermic peaks. Glass transition temperatures (T_g) were read at the middle of the change in heat capacity. Indium and zinc were used as calibration standards. An Olympus BX-40 optical polarized microscope (100× magnification) equipped with a Mettler FP 82 hot stage and a Mettler FP 80 central processor was used to verify thermal transitions and characterize anisotropic textures.[11]

X-ray diffraction experiments on liquid crystal phases were performed using an Image Plate area detector (MAR Research) with a graphite-monochromatized pinhole-collimated beam and a helium tent. The samples, in glass capillaries, were held in a temperature-controlled cell. Densities, ρ, were determined by flotation in DMSO/H_2O (**21-12/0**) and DMSO/CCl_4 (**19-6/6**, **19-4/8**, **21-8/4**, **21-6/6**, **21-4/8**).

Synthesis. The synthesis of $(Ph_3P)_4Pd(0)$,[12] 4-(dimethylamino)pyridinium *p*-toluenesulfonate (DPTS),[13] tetraethylene glycol monoallyl ether (**16**),[14] tetraethylene glycol monomethyl methacrylate (**17**),[9] **11-12/0**,[15] **19-12/0**,[1g] **20-12/0**,[1g] and **21-12/0**[1g] have been described previously.

5-Bromopentan-1-ol (1). A mixture of 1,5-pentanediol (41.7 g, 400 mmol), 800 mL benzene, and 48% HBr (67 mL, 400 mmol) was refluxed and water was azeotropically distilled.[16] After 18 h, benzene was removed by rotary evaporation, and the resulting brown oil was distilled under vacuum to yield 29.5 g (44.2%) of a clear oil. Purity (GLC), 92.7%; bp 83−84 °C/2.5 mmHg (lit.[17] bp 75−76 °C/0.5 mmHg). ^{1}H NMR: 1.56 (m, 4H, $(CH_2)_2CH_2OH$), 1.82 (m, 3H, CH_2CH_2Br), 3.42 (t, 2H, CH_2Br, $J = 6.7$ Hz), 3.66 (t, 2H, CH_2OH, $J = 6.2$ Hz).

1-Bromo-5-(2-tetrahydropyranyloxy)pentane (2). To **1** (29.5 g, 177 mmol), cooled to 0 °C, were added DHP (17.9 g, 213 mmol) and *p*-TsOH (0.40 g, 2.1 mmol) were added.[18] An exothermic reaction occurred. The mixture turned first green and then brown. After the reaction was allowed to warm to room temperature, ^1H NMR analysis indicated complete conversion. However, after vacuum distillation, ^1H NMR analysis showed that 18% of the obtained product was reverted to the starting alcohol. The distilled product (25.0 g, 19.1 mmol of **1**) was cooled to 0 °C, and an additional portion of DHP (3.20 g, 38.1 mmol) and a catalytic amount of *p*-TsOH were added. After 1.5 h at 0 °C, ^1H NMR analysis indicated complete conversion. The mixture was diluted with Et_2O and then washed one time with 5% $NaHCO_3$ and one time with H_2O. The product was dried over $MgSO_4$ and filtered, and the solvent distilled to yield 25.0 g (56.2%) of a clear liquid which was used without further purification. Purity (GLC), 99+%. ^1H NMR: 1.58−1.90 (overlapped peaks, 12H, $OC(H)(CH_2)_3$ and $(CH_2)_3CH_2Br$), 3.38−3.46 (overlapped peaks, 4H, CH_2Br and $CH_2OC(H)O$), 3.73 (m, 2H, $OCH(CH_2)OCH_2$), 4.57 (m, 1H, $OCH(CH_2)O$).

7-Octen-1-ol (3). Magnesium turnings (1.46 g, 60.1 mmol) were covered with 25 mL anhydrous THF, and **2** (12.6 g, 50.2 mmol) was added dropwise until refluxing of the Grignard solution was observed. Addition was continued to maintain the reflux, and the stirring mixture was allowed to cool to room temperature. The Grignard reagent was transferred to an addition funnel under N_2 and added dropwise to a stirring solution of allyl bromide (5.56 g, 46.0 mmol) and Li_2CuCl_4 (1.5 mL of a 0.1 M solution in THF, 0.30 mol %), all in 25 mL of anhydrous THF.[10] The reaction mixture was maintained at −10 °C. After 3 h, the reaction was warmed to room temperature and was diluted with Et_2O. The ether phase was separated and washed with water brine. Then it was dried over $MgSO_4$ and filtered, and the solvent was removed by rotary evaporation to yield 9.5 g (89%) of a light yellow oil. The oil was dissolved in a solution of 1 N HCl in 95% EtOH and refluxed for 3 h, after which time ^1H NMR indicated complete deprotection. The solvent was distilled and the product was purified by vacuum distillation to yield 2.9 g (45%) of a clear oil. Purity (GLC), 97.3%; bp 77−80 °C/4.6 mmHg (lit.[19] bp 94−96 °C/17 mmHg). ^1H NMR: 1.36 (bs, 6H, $(CH_2)_3CH_2CH_2OH$), 1.57 (m, 3H, CH_2CH_2OH), 2.04 (m, 2H, $CH_2{=}CHCH_2$), 3.64 (t, 2H, CH_2OH, $J = 6.6$ Hz), 4.96 (m, 2H, $CH_2{=}CH$), 5.80 (m, 1H, $CH_2{=}CH$); ^{13}C NMR: 25.5 ($CH_2CH_2CH_2OH$), 28.8 ($CH_2{=}CHCH_2CH_2CH_2$), 32.5 (CH_2CH_2OH), 33.6 ($CH_2{=}CHCH_2$), 62.6 (CH_2OH), 114.3 ($CH_2{=}CH$), 138.5 ($CH_2{=}CH$).

1*H*,1*H*,2*H*,2*H*,3*H*,3*H*,4*H*,4*H*,5*H*,5*H*,6*H*,6*H*,7*H*,8*H*,8*H*-Perfluoro-7-iodododecan-1-ol (4). Compound **4** was synthesized by the Pd(0) catalyzed radical addition of *n*-perfluorobutyl iodide to **3**.[20] A solution of **3** (8.0 g, 62 mmol) and 45 mL hexanes was cooled to 0 °C under N_2 in a Schlenk tube. *n*-Perfluorobutyl iodide (22 g, 64 mmol) and $(Ph_3P)_4Pd(0)$ (2.9 g, 4.0 mol %) were added. The heterogeneous orange mixture was allowed to reach room temperature while stirring. The reaction was complete after ^1H NMR. The mixture was filtered and the solids were washed with Et_2O. The solvent was distilled, and the resultant orange oil (26 g, 88%) was used without further purification. ^1H NMR: 1.39 (m, 6H, $(CH_2)_3CH_2CH_2OH$), 1.58 (m, 2H, CH_2CH_2OH), 2.85 (m, 2H, CF_2CH_2), 3.66 (t and bs, 3H, CH_2OH, $J = 6.5$ Hz), 4.33 (m, 1H, $C(H)I$); ^{19}F NMR: −81.6 (m, 3F, CF_3), −114.0 (m, 2F, CF_2CH_2), −125.1 (m, 2F, $CF_2CF_2CH_2$), −126.5 (m, 2F, CF_3CF_2); ^{13}C NMR: 20.7 (CHI), 25.5 ($CH_2CH_2CH_2OH$), 28.3 ($CF_2CH_2CH(I)CH_2$), 29.5 ($CH_2CH_2CH_2CH_2OH$), 32.5 (CH_2CH_2OH), 40.2 ($CF_2CH_2CH(I)CH_2CH_2$), 41.5 (t, CF_2CH_2, $J_{C\text{-}F} = 21.0$ Hz), 62.7 (CH_2OH).

1*H*,1*H*,2*H*,2*H*,3*H*,3*H*,4*H*,4*H*,5*H*,5*H*,6*H*,6*H*,7*H*,7*H*,8*H*,8*H*-Perfluorododecan-1-ol (5-8/4). To a slurry of $LiAlH_4$ (1.18 g, 31.1 mmol) in 12 mL of Et_2O was added dropwise **4** (7.4 g, 16 mmol) to maintain reflux.[21] ^1H NMR and GLC analysis indicated complete conversion in 30 min. The reaction was quenched by successive addition of 1 mL of H_2O, 1 mL of 15% NaOH, and 3 mL of H_2O. The resulting granular salts were filtered and washed with Et_2O. The Et_2O was distilled to yield 5.4 g (100%) of a dark oil (due to traces of palladium). Purity (GLC), 94.9%; bp 96−100 °C/1.0 mmHg. ^1H NMR: 1.34 (bs, 10H, $(CF_2CH_2(CH_2)_5)$, 1.57 (m, 2H, CH_2CH_2OH), 2.01 (m, 2H, CF_2CH_2), 3.65 (t, 2H, CH_2OH, $J = 6.5$ Hz); ^{19}F NMR: −81.6 (m, 3F, CF_3), −115.3 (t, 2F, CF_2CH_2, $J = 14.2$ Hz), −125.1 (s, 2F, $CF_2CF_2CH_2$), −126.7 (m, 2F, CF_3CF_2); ^{13}C NMR: 20.0 ($CF_2CH_2CH_2CH_2$), 25.6 ($CH_2CH_2CH_2OH$), 28.9−29.1 ($CF_2CH_2CH_2CH_2CH_2CH_2$), 31.1 (t, CF_2CH_2, $J_{C\text{-}F} = 22.3$ Hz), 32.6 (CH_2CH_2OH), 62.7 (CH_2OH).

1*H*,1*H*,2*H*,2*H*,3*H*,3*H*,4*H*,4*H*,5*H*,5*H*,6*H*,6*H*,7*H*,7*H*,8*H*,8*H*-Perfluorododecyl Bromide (6-8/4). A mixture of **5-8/4** (4.40 g, 12.6 mmol), Aliquat 336 (0.20 g, 4.0 mol %), and HBr, 48% (4.4 mL, 26 mmol), was heated to 100 °C while stirring.[22] After 12 h, the reaction was complete (GLC). The mixture was cooled to room temperature and extracted with Et_2O. The organic layer was washed three times with H_2O, dried over $MgSO_4$, and filtered, and the solvent was distilled to yield 4.92 g (95.0%) of a light yellow oil. Purity (GLC), 93.5%; bp 85−90 °C/0.40 mmHg. ^1H NMR: 1.36−1.59 (bs, 10H, $(CF_2CH_2(CH_2)_5)$, 1.86 (m, 2H, CH_2CH_2Br), 2.01 (m, 2H, CF_2CH_2), 3.41 (t, 2H, CH_2Br, $J = 6.7$ Hz); ^{19}F NMR: −81.6 (m, 3F, CF_3), −115.2 (m, 2F, CF_2CH_2), −125.0 (s, 2F, $CF_2CF_2CH_2$), −126.6 (m, 2F, CF_3CF_2); ^{13}C NMR: 20.0 ($CF_2CH_2CH_2CH_2$), 28.0 ($CH_2CH_2CH_2Br$), 28.5 ($CF_2CH_2CH_2CH_2$), 29.0 ($CF_2(CH_2)_3CH_2CH_2$), 30.7 (t, CF_2CH_2, $J_{C\text{-}F} = 22.5$ Hz), 32.7 (CH_2CH_2Br), 33.7 (CH_2Br).

2*H*,2*H*,3*H*,4*H*,4*H*-Perfluoro-3-iodododecanoic Acid (8). Following the procedure used for **4**, from **7** (2.73 g, 31.7 mmol) and *n*-perfluorooctyl iodide (15.8 g, 28.9 mmol) was obtained 13.2 g (72.3%) of an orange powder. **8** was used without purification even though ^1H NMR analysis indicated the presence of a trace of **7**. ^1H NMR: 3.02 (dq, 2H, CF_2CH_2, $J_{H\text{-}F} = 17.5$ Hz, $J_{H\text{-}H} = 8.4$ Hz), 3.17 (d, 1H, $CH(I)CH_a(H_b)CO_2H$, $J_{H\text{-}Ha} = 8.1$ Hz), 3.23 (d, 1H, $CH(I)CH_a(H_b)CO_2H$, $J_{H\text{-}Hb} = 4.9$ Hz), 4.57 (m, 1H, CHI). ^{19}F NMR: −81.3 (t, 3F, CF_3, $J_{F\text{-}F} = 9.9$ Hz), −114.6 (m, 2F, CF_2CH_2), −122.5 (m, 8F, $((CF_2)_4CF_2CH_2)$, −124.1 (s, 2F, $CF_3CF_2CF_2$), −126.7 (s, 2F, CF_3CF_2); ^{13}C NMR: 7.82 (s, CHI), 40.6 (t, CF_2CH_2, $J_{C\text{-}F} = 20.0$ Hz), 45.0 (s, CH_2CO_2H), 175.1 (s, CO_2H).

1*H*,1*H*,2*H*,2*H*,3*H*,3*H*,4*H*,4*H*-Perfluorododecan-1-ol (5-4/8). Compound **5-4/8** was synthesized by the one pot reduction of halide and carboxylic acid of **8** with $LiAlH_4$ according to the procedure used for **5-8/4**. THF was used as solvent. From **8** (13.0 g, 20.5 mmol) and $LiAlH_4$ (3.11 g, 82.0 mmol), 6.68 g (66.2%) of **5-4/8** as a white, waxy solid was obtained after sublimation at 40 °C. Purity (GLC), 99.6%; mp 42−44 °C (lit.[23] mp unreported). ^1H NMR: 1.66 (m, 4H, $CF_2CH_2CH_2CH_2$), 2.12 (m, 2H, CF_2CH_2), 3.71 (t, 2H, CH_2OH, $J = 5.9$ Hz); ^{19}F NMR: −81.3 (t, 3F, CF_3, $J = 10.2$ Hz), −115.1 (t, 2F, CF_2CH_2, $J = 13.7$ Hz), −122.5 (s, 6F, $((CF_2)_3CF_2CH_2)$, −123.3 (s, 2F, $CF_3CF_2CF_2CF_2$), −124.1 (s, 2F, $CF_3CF_2CF_2$), −126.7 (s, 2F, CF_3CF_2); ^{13}C NMR: 16.8 ($CF_2CH_2CH_2$), 30.6 (t, CF_2CH_2, $J_{C\text{-}F} = 22.2$ Hz), 31.9 (CH_2CH_2OH), 62.1 (CH_2OH).

1*H*,1*H*,2*H*,2*H*,3*H*,3*H*,4*H*,4*H*-Perfluorododecyl Bromide (6-4/8). Compound **6-4/8** was obtained from **5-4/8** by the procedure described for the synthesis of **6-8/4**. From **5-4/8** (6.50 g, 13.2 mmol), Aliquat 336 (0.21 g, 4 mol %), and 48% HBr (8.0 mL, 47 mmol) was obtained 5.81 g (79.3%) of white, needle-like crystals after sublimation at room temperature. Purity (GLC), 98.3%; mp 31−33 °C. ^1H NMR: 1.75−2.16 (overlapped peaks, 6H, $CF_2CH_2CH_2CH_2$), 3.44 (t, 2H, CH_2Br, $J = 6.5$ Hz); ^{19}F NMR: −81.3 (t, 3F, CF_3, $J_{F\text{-}F} = 10.0$ Hz), −114.9 (t, 2F, CF_2CH_2, $J_{F\text{-}F} = 13.0$ Hz), −122.4 (m, 6F, $((CF_2)_3CF_2CH_2)$, −123.3 (s, 2F, $CF_3CF_2CF_2CF_2$), −124.0 (s, 2F, $CF_3CF_2CF_2$), −126.6 (s, 2F, CF_3CF_2); ^{13}C NMR: 19.1 ($CF_2CH_2CH_2$), 30.1 (t, CF_2CH_2, $J_{C\text{-}F} = 23.0$ Hz), 31.9 (CH_2CH_2Br), 32.3 (CH_2Br).

Methyl 3,4,5-Tris(1*H*,1*H*,2*H*,2*H*,3*H*,3*H*,4*H*,4*H*,5*H*,5*H*,6*H*,6*H*,7*H*,7*H*,8*H*,8*H*-perfluorododecan-1-yloxy)benzoate (10-8/4). Compound **10-8/4** was synthesized by the procedure for the alkylation of methyl 3,4,5-trihydroxybenzoate (**9**) with alkyl bromides.[15] To a mixture of K_2CO_3 (3.2 g, 23 mmol) and 60 mL of DMF under N_2 was added **9** (0.47 g, 2.6 mmol). **6-8/4** (3.7 g, 9.0 mmol) at 65 °C was added, and the solution turned brown. The mixture was stirred at 65 °C for 2 h (complete conversion by TLC). The mixture was poured into 200 mL of ice water and was acidified with concentrated HCl. The aqueous mixture was extracted with Et_2O. The organic layer was washed two times with H_2O, dried over $MgSO_4$, and filtered, and the solvent was distilled. Purification by flash chromatography (basic Al_2O_3, CH_2Cl_2) yielded 2.3 g (77%) of a clear oil. Purity (HPLC), 99+%; TLC (10:1 hexanes/ethyl acetate), $R_f = 0.35$. ^{1}H NMR: 1.37−1.48 (bs, 30H, ($CF_2CH_2(CH_2)_5$), 1.82 (m, 6H, CH_2CH_2OAr), 2.05 (m, 6H, CF_2CH_2), 3.89 (s, 3H, CH_3), 4.01 (t, 6H, CH_2OAr, $J = 6.3$ Hz), 7.26 (s, 2H, *ortho* to CO_2CH_3); ^{19}F NMR: −81.7 (m, 9F, CF_3), −115.2 (m, 6F, CF_2CH_2), −125.1 (s, 6F, $CF_2CF_2CH_2$), −126.7 (m, 6F, CF_3CF_2); ^{13}C NMR: 20.1 ($CF_2CH_2CH_2CH_2$), 26.0 ($CH_2CH_2CH_2OAr$), 29.1−29.3 ($CF_2(CH_2)_3CH_2CH_2$), 30.3 (CH_2CH_2OAr), 30.8 ($CF_2CH_2CH_2CH_2$), 31.2 (t, CF_2CH_2, $J = 22.5$ Hz), 52.1 (CH_3), 69.1 (CH_2OAr, 3,5-position), 73.3 (CH_2OAr, 4-position), 108.0 (*ortho* to CO_2CH_3), 124.6 (*ipso* to CO_2CH_3), 142.1 (*ipso* to oxygen on 4-position), 152.6 (*ipso* to oxygen on 3,5-position), 166.8 (CO_2).

3,4,5-Tris(1*H*,1*H*,2*H*,2*H*,3*H*,3*H*,4*H*,4*H*,5*H*,5*H*,6*H*,6*H*,7*H*,7*H*,8*H*,8*H*-perfluorododecan-1-yloxy)benzoic Acid (11-8/4). To **10-8/4** (2.1 g, 1.8 mmol) in 21 mL of 95% EtOH was added 2 mL of 10 N aqueous KOH solution and the reaction was heated to reflux. After 2 h, the hydrolysis was complete (TLC). The mixture was concentrated on a rotary evaporator, and THF was added to form a solution. This solution was acidified with concentrated HCl. Additional THF was added to maintain the solution. The solvent was distilled, and the product was dissolved in Et_2O, washed two times with H_2O, and dried over $MgSO_4$. After filtration, the solvent was distilled to yield 1.9 g (91%) of a white, waxy product. Purity (HPLC), 99+%; TLC (CH_2Cl_2), $R_f = 0.25$. Thermal transitions are recorded in Table 1. ^{1}H NMR: 1.38−1.49 (bs, 30H, ($CF_2CH_2(CH_2)_5$), 1.79 (m, 6H, CH_2CH_2OAr), 2.05 (m, 6H, CF_2CH_2), 4.03 (overlapped t, 6H, CH_2OAr, $J = 6.3$ Hz), 7.32 (s, 2H, *ortho* to CO_2H); ^{19}F NMR: −81.7 (m, 9F, CF_3), −115.3 (m, 6F, CF_2CH_2), −125.1 (m, 6F, $CF_2CF_2CH_2$), −126.7 (m, 6F, CF_3CF_2); ^{13}C NMR: 20.1 ($CF_2CH_2CH_2CH_2$), 26.0 ($CH_2CH_2CH_2OAr$), 29.1−29.2 ($CF_2(CH_2)_3CH_2CH_2$), 30.3 (CH_2CH_2OAr), 30.8 ($CF_2CH_2CH_2CH_2$), 31.2 (t, CF_2CH_2, $J_{C\text{-}F} = 22.6$ Hz), 69.1 (CH_2OAr, 3,5-position), 73.5 (CH_2OAr, 4-position), 108.6 (*ortho* to CO_2H), 123.9 (*ipso* to CO_2H), 143.2 (*ipso* to oxygen on 4-position), 152.9 (*ipso* to oxygen on 3,5-position), 172.2 (CO_2).

Methyl 3,4,5-Tris(1*H*,1*H*,2*H*,2*H*,3*H*,3*H*,4*H*,4*H*-perfluorododecan-1-yloxy)benzoate (10-4/8). To a mixture of K_2CO_3 (3.11 g, 22.5 mmol) and 60 mL DMF under Ar was added **9** (0.47 g, 2.5 mmol). The mixture was heated to 60 °C, and subsequently **6-4/8** (5.6 g, 10 mmol) was added. After 8 h (complete by TLC), the mixture was poured into 600 mL of ice water. The crude product was recrystallized from acetone to yield 3.44 g (85.7%) of a cream colored powder. Purity (HPLC), 100%; mp 59−63.5 °C; TLC (3:1 hexanes/ethyl acetate), $R_f = 0.5$. ^{1}H NMR: 1.89 (m, 12H, $CF_2CH_2(CH_2)_2$), 2.17 (m, 6H, CF_2CH_2), 3.90 (s, 3H, CH_3), 4.07 (overlapped t, 6H, CH_2OAr), 7.28 (s, 2H, *ortho* to CO_2CH_3); ^{19}F NMR: −81.4 (overlapped t, 9F, CF_3), −115.1 (m, 6F, CF_2CH_2), −122.6 (m, 18F, $(CF_2)_3CF_2CH_2$), −123.4 (s, 6F, $CF_3(CF_2)_2CF_2$), −124.1 (s, 6F, $CF_3CF_2CF_2$), −126.8 (m, 6F, CF_3CF_2); ^{13}C NMR: 17.2 ($CF_2CH_2CH_2$, 4-position), 17.3 ($CF_2CH_2CH_2$, 3,5-position), 28.7 (CH_2CH_2OAr), 29.7−30.6 (overlapped t, CF_2CH_2, 4-position and 3,5-position), 52.2 (CH_3), 68.4 (CH_2OAr, 3,5-position), 72.7 (CH_2OAr, 4-position), 108.1 (*ortho* to CO_2CH_3), 125.3 (*ipso* to CO_2CH_3), 141.9 (*ipso* to oxygen, 4-position), 152.6 (*ipso* to oxygen, 3,5-position), 166.6 (CO_2).

3,4,5-Tris(1*H*,1*H*,2*H*,2*H*,3*H*,3*H*,4*H*,4*H*-perfluorododecan-1-yloxy)benzoic Acid (11-4/8). Basic hydrolysis of **10-4/8** (3.34 g, 2.08 mmol) yielded 3.3 g (100%) of a light yellow powder after precipitation of its THF solution into 1000 mL of ice water. Thermal transitions are recorded in Table 1. ^{1}H NMR ($CDCl_3$/Freon 113): 1.95 (m, 12H, $CF_2CH_2(CH_2)_2$), 2.21 (m, 6H, CF_2CH_2), 4.13 (overlapped t, 6H, CH_2OAr), 7.41 (s, 2H, *ortho* to CO_2H); ^{13}C NMR ($CDCl_3$/Freon 113): 17.9 ($CF_2CH_2CH_2$), 29.3 (CH_2CH_2OAr), 31.2 (overlapped t, CF_2CH_2, 4- and 3,5-position), 68.9 (CH_2OAr, 3,5-position), 73.0 (CH_2OAr, 4-position), 109.3 (*ortho* to CO_2H), 125.0 (*ipso* to CO_2H), 143.5 (*ipso* to oxygen, 4-position), 153.3 (*ipso* to oxygen, 3,5-position), 172.4 (CO_2).

1-Bromohex-5-ene (13). Compound **13** was synthesized by the mono-elimination of HBr from 1,6-dibromohexane (**12**) in HMPA.[24] **12** (47.7 g, 196 mmol) was heated to 185−190 °C, and HMPA (45.0 mL, 259 mmol) was added dropwise. The addition was controlled in such a way as to maintain slow distillation (~1 drop/s) of the elimination product. The alkene was collected by distillation at 130−150 °C (lit.[25] bp 47−51 °C/16 mmHg). After complete addition of HMPA, the pot was cooled to room temperature. **13** was purified by distillation at 145−150 °C to yield 13.1 g (41.0%) of a clear oil. Purity (GLC), 99+%; ^{1}H NMR: 1.54 (m, 2H, $CH_2{=}CHCH_2CH_2$), 1.88 (m, 2H, CH_2CH_2Br), 2.07 (m, 2H, $CH_2{=}CHCH_2$), 3.42 (t, 2H, CH_2Br, $J = 6.7$ Hz), 5.00 (m, 2H, $CH_2{=}CH$), 5.81 (m, 1H, $CH_2{=}CH$).

Methyl 3,4,5-Tris(hex-5-en-1-yloxy)benzoate (14). From **9** (7.6 g, 41 mmol) and **13** (20.0 g, 123 mmol) was obtained 14.5 g (82.1%) of a clear oil by following the procedure used for **10-8/4**. Purity (HPLC), 99+%; TLC (CH_2Cl_2), $R_f = 0.7$. ^{1}H NMR: 1.59 (m, 6H, $CH_2{=}CHCH_2CH_2$), 1.84 (m, 6H, CH_2CH_2O), 2.12 (m, 6H, $CH_2{=}CHCH_2$), 3.90 (s, 3H, CH_3), 4.03 (t, 6H, CH_2O, $J = 6.3$ Hz), 5.00 (m, 2H, $CH_2{=}CH$), 5.82 (m, 1H, $CH_2{=}CH$), 7.26 (s, 2H, *ortho* to CO_2CH_3).

Methyl 3,4,5-Tris(1*H*,1*H*,2*H*,2*H*,3*H*,3*H*,4*H*,4*H*,5*H*,6*H*,6*H*-perfluoro-5-iodododecan-1-yloxy)benzoate (15). Compound **15** was made by the procedure used for **4**. From **14** (1.00 g, 2.32 mmol) and *n*-perfluorohexyl iodide (4.14 g, 9.29 mmol) was obtained 3.30 g (80.4%) of a dark orange oil. Purity (HPLC), 99+%; TLC (CH_2Cl_2), $R_f = 0.9$. ^{1}H NMR: 1.50−1.86 (m, 18H, $(CH_2)_3CH_2OAr$), 2.88 (m, 6H, CF_2CH_2), 3.90 (s, 3H, CH_3), 4.07 (overlapped t, 6H, CH_2OAr), 4.37 (m, 3H, CHI), 7.28 (s, 2H, *ortho* to CO_2CH_3).

3,4,5-Tris(1*H*,1*H*,2*H*,2*H*,3*H*,3*H*,4*H*,4*H*,5*H*,5*H*,6*H*,6*H*-perfluorododecan-1-yloxy)benzoic Acid (11-6/6). Compound **11-6/6** was prepared in two steps by the reduction of **15** with *n*-Bu_3SnH[26] followed by basic hydrolysis. To a solution of **15** (8.1 g, 4.6 mmol) in 100 mL of benzene was added AIBN (74.0 mg, 0.46 mmol), and the mixture was heated to 70 °C under Ar. *n*-Bu_3SnH (7.50 mL, 28.3 mmol) was added dropwise *via* a syringe. After 14 h at 70 °C, ^{1}H NMR analysis indicated 53% conversion. AIBN (40 mg, 0.25 mmol) and *n*-Bu_3SnH (4.60 g, 15.8 mmol) were added. After this addition, the reaction was complete (^{1}H NMR). Benzene was distilled to yield a two layer mixture. The heavier layer was solidified by immersion in a dry ice−acetone bath. On warming to room temperature, the lighter oil layer was decanted and found to contain mostly Sn based byproducts with only a trace of product. Conversely, the recovered fraction consisted of predominantly product with only traces of Sn byproducts. The solid product was hydrolyzed as described for **10-8/4**. After three recrystallizations from 95% EtOH, 3.5 g (56%) of a white powder was obtained. Purity (HPLC), 99+%. Thermal transitions and corresponding enthalpy changes are recorded in Table 1. ^{1}H NMR: 1.50 (m, 18H, $(CH_2)_3CH_2CH_2OAr$), 1.84 (m, 6H, CH_2CH_2OAr), 2.06 (m, 6H, CF_2CH_2), 4.04 (overlapped t, 6H, CH_2OAr, $J = 6.1$ Hz), 7.32 (s, 2H, *ortho* to CO_2H); ^{19}F NMR: −81.4 (t, 9F, CF_3, $J = 9.4$ Hz), −115.1 (m, 6F, CF_2CH_2), −122.6 (m, 6F, $CF_2CF_2CH_2$), −123.6 (m, 6F, $CF_3(CF_2)_2CF_2$), −124.2 (m, 6F, $CF_3CF_2CF_2$), −126.8 (m, 6F, CF_3CF_2); ^{13}C NMR: 20.6 ($CF_2CH_2CH_2$), 26.3 ($CH_2CH_2CH_2OAr$), 29.3 (CH_2CH_2OAr, 3,5-position), 29.5 (CH_2CH_2OAr, 4-position), 29.6 ($CF_2CH_2CH_2CH_2$, 3,5-position), 30.6 ($CF_2CH_2CH_2CH_2$, 4-position), 31.3 (t, CF_2CH_2, $J_{C\text{-}F} = 22.5$ Hz), 69.4 (CH_2OAr, 3,5-position), 73.7 (CH_2OAr, 4-position), 109.1 (*ortho* to CO_2H), 124.4 (*ipso* to CO_2H), 143.4 (*ipso* to oxygen, 4-position), 153.3 (*ipso* to oxygen, 3,5-position), 172.5 (CO_2).

2-{2-[2-(2-Hydroxyethoxy)ethoxy]ethoxy}ethyl 3,4,5-Tris(1*H*,1*H*,2*H*,2*H*,3*H*,3*H*,4*H*,4*H*,5*H*,5*H*,6*H*,6*H*,7*H*,7*H*,8*H*,8*H*-perfluorododecan-1-yloxy)benzoate (19-8/4). Compound **19-8/4** was synthesized in three steps by the conversion of **11-8/4** to the acid chloride, its esterification with tetraethylene glycol monoallyl ether (**16**)[14] in pyridine, and cleavage of the allyl ether with *p*-TsOH in the presence of Pd on carbon.[27] Only the final product, **19-8/4**, was fully characterized. To a solution of **11-8/4** (2.8 g, 2.4 mmol) in 30 mL of anhydrous CH_2Cl_2 was added a few drops of DMF and $SOCl_2$ (1 mL, excess). After 1 h, the reaction was complete (IR, shift of the carbonyl absorption from 1678 to 1745 cm^{-1}). The solvent and excess $SOCl_2$ were distilled, and the oily product was dried under high vacuum to yield 2.8 g (100%) of the acid chloride as a clear oil. The product was used without further purification. A flame-dried round bottom flask equipped with a magnetic stirrer and inert gas inlet–outlet was charged with **16** (0.70 g, 3.0 mmol) dissolved in 18 mL of dry pyridine. A solution of acid chloride (1.8 g, 1.5 mmol) in 2 mL of anhydrous CH_2Cl_2 was added slowly and the mixture stirred at room temperature. After 16 h, two spots were observed on the TLC plate corresponding to **18-8/4** and **11-8/4**. The mixture was poured into water and extracted two times with Et_2O. The organic layer was washed with 10% HCl and H_2O, dried over $MgSO_4$, and filtered, and the solvent was distilled. To a mixture of the resultant oil (1.8 g) in 20 mL of 90% MeOH were added 5% Pd on carbon (0.18 g, 10 wt %) and *p*-TsOH (0.02 g, 1.0 wt %). The mixture was refluxed, and after 2 h, ^1H NMR indicated complete deprotection. The mixture was taken up in THF and filtered to remove carbon, and the solvent was distilled. The resultant crude product was purified by flash chromatography (basic Al_2O_3, ethyl acetate/THF gradient) to yield 0.90 g (45%) of a clear oil. Purity (HPLC), 99+%; TLC (ethyl acetate), $R_f = 0.5$. Thermal transitions are summarized in Table 1. ^1H NMR: 1.38 (m, 30H, $(CH_2)_5CH_2CH_2OAr$), 1.78 (m, 6H, CH_2CH_2OAr), 2.05 (m, 6H, CF_2CH_2), 2.47 (bs, 1H, O*H*), 3.57–3.69 (overlapped peaks, 12H, $CO_2CH_2CH_2(OCH_2CH_2)_3OH$), 3.83 (t, 2H, $CO_2CH_2CH_2$, $J = 5.0$ Hz), 4.01 (t, 6H, CH_2OAr, $J = 6.2$ Hz), 4.47 (t, 2H, CO_2CH_2, $J = 4.9$ Hz), 7.27 (s, 2H, *ortho* to CO_2); ^{19}F NMR: −81.7 (m, 9F, CF_3), −115.3 (m, 6F, CF_2CH_2), −125.1 (m, 6F, $CF_2CF_2CH_2$), −126.7 (m, 6F, CF_3CF_2); ^{13}C NMR: 20.6 (t, $CF_2CH_2CH_2CH_2$, $J_{C\text{-}F} = 3.7$ Hz), 26.7 ($CH_2CH_2CH_2OAr$), 29.6–29.8 ($CF_2(CH_2)_3CH_2CH_2CH_2CH_2$), 30.8 ($CF_2CH_2CH_2CH_2$), 31.3 (t, CF_2CH_2, $J = 22.1$ Hz), 62.2 (CH_2OH), 64.6 (CO_2CH_2), 69.7 (CH_2OAr, 3,5-position), 69.9–73.1 ($CH_2O(CH_2CH_2O)_3CH_2$), 73.9 (CH_2OAr, 4-position), 108.8 (*ortho* to CO_2), 125.3 (*ipso* to CO_2), 143.0 (*ipso* to oxygen on 4-position), 153.4 (*ipso* to oxygen on 3,5-position), 167.0 (CO_2).

2-{2-[2-(2-(Methacryloyloxy)ethoxy)ethoxy]ethoxy}ethyl 3,4,5-Tris(1*H*,1*H*,2*H*,2*H*,3*H*,3*H*,4*H*,4*H*,5*H*,5*H*,6*H*,6*H*,7*H*,7*H*,8*H*,8*H*-perfluorododecan-1-yloxy)benzoate (20-8/4). To a solution of **19-8/4** (0.90 g, 0.67 mmol) in 10 mL of anhydrous CH_2Cl_2 under Ar was added Et_3N (0.53 g, 5.3 mmol). Methacryloyl chloride (0.21 g, 2.0 mmol) was added dropwise *via* a syringe to the reaction mixture at 0 °C, and the mixture was allowed to warm to room temperature. After 2 h, the mixture was filtered to remove $Et_3NH^+Cl^-$ and the solvent was distilled. The product was dissolved in Et_2O, washed three times with 10% HCl and two times with H_2O, and dried over $MgSO_4$. After the solvent was evaporated, a light yellow oil was obtained which was purified by flash chromatography (basic Al_2O_3, ethyl acetate/THF gradient) to yield 0.42 g (45%) of a clear oil. Purity (HPLC), 99+%; TLC (2:1 hexanes/ethyl acetate), $R_f = 0.5$. ^1H NMR: 1.38–1.48 (overlapped peaks, 30H, $CF_2CH_2(CH_2)_5$), 1.78 (m, 6H, CH_2CH_2OAr), 1.94 (s, 3H, $CH_2{=}C(CH_3)$), 2.01 (m, 6H, CF_2CH_2), 3.65–3.73 (overlapped peaks, 10H, $ArCO_2CH_2CH_2(OCH_2CH_2)_2OCH_2CH_2$), 3.82 (t, 2H, $ArCO_2CH_2CH_2$, $J = 4.8$ Hz), 4.01 (t, 6H, CH_2OAr, $J = 6.4$ Hz), 4.30 (t, 2H, $CH_2O_2CC(CH_3){=}CH_2$, $J = 4.9$ Hz), 4.46 (t, 2H, $ArCO_2CH_2$, $J = 4.8$ Hz), 5.57 (s, 1H, $CH_2{=}C(CH_3)$, *trans* to C=O), 6.12 (s, 1H, $CH_2{=}C(CH_3)$, *cis* to C=O), 7.27 (s, 2H, *ortho* to CO_2); ^{19}F NMR: −81.7 (m, 9F, CF_3), −115.8 (m, 6F, CF_2CH_2), −125.2 (m, 6F, $CF_2CF_2CH_2$), −126.7 (m, 6F, CF_3CF_2); ^{13}C NMR: 18.2 (CH_3), 20.0 ($CF_2CH_2CH_2CH_2$), 25.9 ($CH_2CH_2CH_2OAr$), 29.0–29.2 ($CF_2(CH_2)_3CH_2CH_2CH_2CH_2$), 30.2 ($CF_2CH_2CH_2CH_2$), 30.7 (t, CF_2CH_2, $J = 22.6$ Hz), 63.8 (CH_2OH), 64.0 (CO_2CH_2), 69.1 (CH_2OAr, 3,5-position), 69.3–70.6 ($CH_2O(CH_2CH_2O)_3CH_2$), 73.3 (CH_2OAr, 4-position), 108.2 (*ortho* to CO_2), 124.7 ($CH_2{=}C(CH_3)$), 125.6 (*ipso* to CO_2), 136.1 ($CH_2{=}C(CH_3)$), 142.4 (*ipso* to oxygen on 4-position), 152.7 (*ipso* to oxygen on 3,5-position), 166.3–167.3 (CO_2).

2-{2-[2-(2-Hydroxyethoxy)ethoxy]ethoxy}ethyl 3,4,5-Tris(1*H*,1*H*,2*H*,2*H*,3*H*,3*H*,4*H*,4*H*,5*H*,5*H*,6*H*,6*H*-perfluorododecan-1-yloxy)benzoate (19-6/6). To a solution of **11-6/6** (1.68 g, 1.22 mmol), **16** (0.30 g, 1.28 mmol), and DPTS (71 mg, 0.24 mmol) in 17 mL of anhydrous CH_2Cl_2 was added DCC (0.34 g, 1.6 mmol), and the reaction was stirred for 16 h.[13] The mixture was diluted with hexanes and filtered to remove the insoluble dicyclohexylurea. The solvent was distilled, and the resultant oil (1.9 g) was purified by column chromatography (SiO_2, 2:1 hexanes/ethyl acetate) to afford 1.1 g (56%) of a clear oil. The allyl ether group of **18-6/6** was cleaved as in the case of **18-8/4**. From **18-6/6** (1.1 g, 0.69 mmol), 5% Pd on carbon (0.11 g, 10 wt %), and *p*-TsOH (25 mg, 0.11 mmol) was obtained 0.55 g (51%) of **19-6/6** after flash column chromatography (SiO_2, 2:1 ethyl acetate:hexanes). Purity (HPLC), 99+%; TLC (2:1 ethyl acetate:hexanes), $R_f = 0.2$. Thermal transitions are recorded in Table 1. ^1H NMR: 1.51 (m, 18H, $CF_2CH_2(CH_2)_3$), 1.84 (m, 6H, CH_2CH_2OAr), 2.07 (m, 6H, CF_2CH_2), 2.50 (bs, 1H, O*H*), 3.60–3.83 (overlapped peaks, 14H, $CO_2CH_2CH_2(OCH_2CH_2)_3OH$), 4.03 (overlapped t, 6H, CH_2OAr), 4.47 (t, 2H, CO_2CH_2, $J = 5.0$ Hz), 7.28 (s, 2H, *ortho* to CO_2); ^{19}F NMR: −81.4 (t, 9F, CF_3, $J = 9.5$ Hz), −115.1 (m, 6F, CF_2CH_2), −122.6 (m, 6F, $CF_2CF_2CH_2$), −123.6 (m, 6F, $CF_3(CF_2)_2CF_2$), −124.2 (m, 6F, $CF_3CF_2CF_2$), −126.8 (m, 6F, CF_3CF_2); ^{13}C NMR: 20.0 ($CF_2CH_2CH_2$), 25.8 ($CH_2CH_2CH_2OAr$), 28.8 (CH_2CH_2OAr, 3,5-position), 28.9 (CH_2CH_2OAr, 4-position), 29.0 ($CF_2CH_2CH_2CH_2$, 3,5-position), 30.0 ($CF_2CH_2CH_2CH_2$, 4-position), 30.7 (t, CF_2CH_2, $J_{C\text{-}F} = 22.3$ Hz), 61.6 (CH_2OH), 64.0 (CO_2CH_2), 68.9 (CH_2OAr, 3,5-position), 69.3–72.5 ($CH_2O(CH_2CH_2O)_3CH_2$), 73.1 (CH_2OAr, 4-position), 108.2 (*ortho* to CO_2H), 124.9 (*ipso* to CO_2H), 142.2 (*ipso* to oxygen, 4-position), 152.7 (*ipso* to oxygen, 3,5-position), 166.3 (CO_2).

2-{2-[2-(2-(Methacryloyloxy)ethoxy)ethoxy]ethoxy}ethyl 3,4,5-Tris(1*H*,1*H*,2*H*,2*H*,3*H*,3*H*,4*H*,4*H*,5*H*,5*H*,6*H*,6*H*-perfluorododecan-1-yloxy)benzoate (20-6/6). From **11-6/6** (2.0 g, 1.5 mmol), **17** (0.41 g, 1.6 mmol), DPTS (0.27 g, 0.91 mmol), and DCC (0.41 g, 2.0 mmol) in 20 mL of anhydrous CH_2Cl_2 was obtained 1.3 g (53%) as a clear oil after purification by flash chromatography (SiO_2, 2:1 hexanes/ethyl acetate).[9] Purity (HPLC), 99+%; TLC (2:1 hexanes/ethyl acetate), $R_f = 0.5$. ^1H NMR: 1.51 (m, 18H, $CF_2CH_2(CH_2)_3$), 1.84 (m, 6H, CH_2CH_2OAr), 1.94 (CH_3), 2.07 (m, 6H, CF_2CH_2), 3.66–3.73 (overlapped peaks, 10H, $CH_2{=}C(CH_3)CO_2CH_2CH_2(OCH_2CH_2)_2$), 3.82 (t, 2H, $ArCO_2CH_2CH_2$, $J = 4.6$ Hz), 4.02 (t, 6H, CH_2OAr, $J = 6.0$ Hz), 4.29 (t, 2H, $CH_2{=}C(CH_3)CO_2CH_2$, $J = 4.9$ Hz), 4.46 (t, 2H, $ArCO_2CH_2$, $J = 4.9$ Hz), 5.57 (s, 1H, $CH_2{=}C(CH_3)$, *trans* to C=O), 6.13 (s, 1H, $CH_2{=}C(CH_3)$, *cis* to C=O), 7.27 (s, 2H, *ortho* to CO_2); ^{19}F NMR: −81.4 (m, 9F, CF_3), −115.1 (m, 6F, CF_2CH_2), −122.6 (m, 6F, $CF_2CF_2CH_2$), −123.5 (s, 6F, $CF_3CF_2CF_2CF_2$), −124.2 (s, 6F, $CF_3CF_2CF_2$), −126.8 (m, 6F, CF_3CF_2); ^{13}C NMR: 18.1 ($CH_2{=}C(CH_3)$), 20.0 ($CF_2CH_2CH_2$), 25.8 ($CH_2CH_2CH_2OAr$), 28.8 (CH_2CH_2OAr, 3,5-position), 28.9 (CH_2CH_2OAr, 4-position), 29.0 ($CF_2CH_2CH_2CH_2$, 3,5-position), 30.0 ($CF_2CH_2CH_2CH_2$, 4-position), 30.7 (t, CF_2CH_2, $J_{C\text{-}F} = 22.0$ Hz), 63.8 ($CH_2{=}C(CH_3)CO_2CH_2$), 64.0 ($ArCO_2CH_2$), 68.8 (CH_2OAr, 3,5-position), 69.2–72.5 ($CH_2O(CH_2CH_2O)_3CH_2$), 73.1 (CH_2OAr, 4-position), 108.1 (*ortho* to CO_2), 124.9 (*ipso* to CO_2), 125.6 ($CH_2{=}C(CH_3)$), 136.0 ($CH_2{=}C(CH_3)$), 142.2 (*ipso* to oxygen, 4-position), 152.7 (*ipso* to oxygen, 3,5-position), 166.3 ($ArCO_2$), 167.3 ($CH_2{=}C(CH_3)CO_2$).

2-{2-[2-(2-Hydroxyethoxy)ethoxy]ethoxy}ethyl 3,4,5-Tris(1*H*,1*H*,2*H*,2*H*,3*H*,3*H*,4*H*,4*H*-perfluorododecan-1-yloxy)benzoate (19-4/8). Following the procedure for **19-6/6**, from **11-4/8** (1.2 g, 0.75 mmol) and **16** (0.25 g, 1.1 mmol) in 1:1 Freon 113:CH_2Cl_2 at 45 °C was obtained 0.90 g (66%) of **18-4/8** as a clear oil (flash column chromatography; SiO_2, 1:1 hexanes/ethyl acetate). After deprotection and purification (flash column chromatography; SiO_2, 2:1 ethyl acetate:hexanes), 0.56 g (64%) of **19-4/8** was obtained as a white, waxy solid. Purity (HPLC), 99+%; TLC (ethyl acetate), $R_f = 0.45$. Thermal transitions are presented in Table 1. ^1H NMR: 1.89 (m, 12H, $CF_2CH_2(CH_2)_2CH_2$), 2.17 (m, 6H, CF_2CH_2), 2.60 (bs, 1H, O*H*), 3.57–3.69 (overlapped peaks, 12H, $CO_2CH_2CH_2(OCH_2CH_2)_3OH$), 3.83 (t, 2H, $CO_2CH_2CH_2$, $J = 4.9$ Hz), 4.08 (overlapped t, 6H, CH_2OAr), 4.48 (t, 2H, CO_2CH_2, $J = 4.8$ Hz), 7.29 (s, 2H, *ortho* to CO_2). ^{19}F NMR: −81.4 (m, 9F, CF_3), −115.1 (m, 6F, CF_2CH_2), −122.6 (m, 18F, $(CF_2)_3CF_2CH_2$), −123.4 (s, 6F, $CF_3CF_2CF_2CF_2$), −124.1 (s, 6F, $CF_3CF_2CF_2$), −126.8 (m, 6F, CF_3CF_2); ^{13}C NMR: 17.1 ($CF_2CH_2CH_2$, 4-position), 17.3 ($CF_2CH_2CH_2$, 3,5-position), 28.7 (CH_2CH_2OAr, 3,5-position), 29.7 (CH_2CH_2OAr, 4-position), 31.0 (t, CF_2CH_2, $J_{C\text{-}F} = 22.0$ Hz), 61.7 (CH_2OH), 64.1 (CO_2CH_2), 68.5 (CH_2OAr, 3,5-position), 69.3–72.5 ($CH_2O(CH_2CH_2O)_3CH_2$), 72.6 (CH_2OAr, 4-position), 108.2 (*ortho* to CO_2), 125.2 (*ipso* to CO_2), 142.0 (*ipso*

Scheme 1. Synthesis of 6-m/n

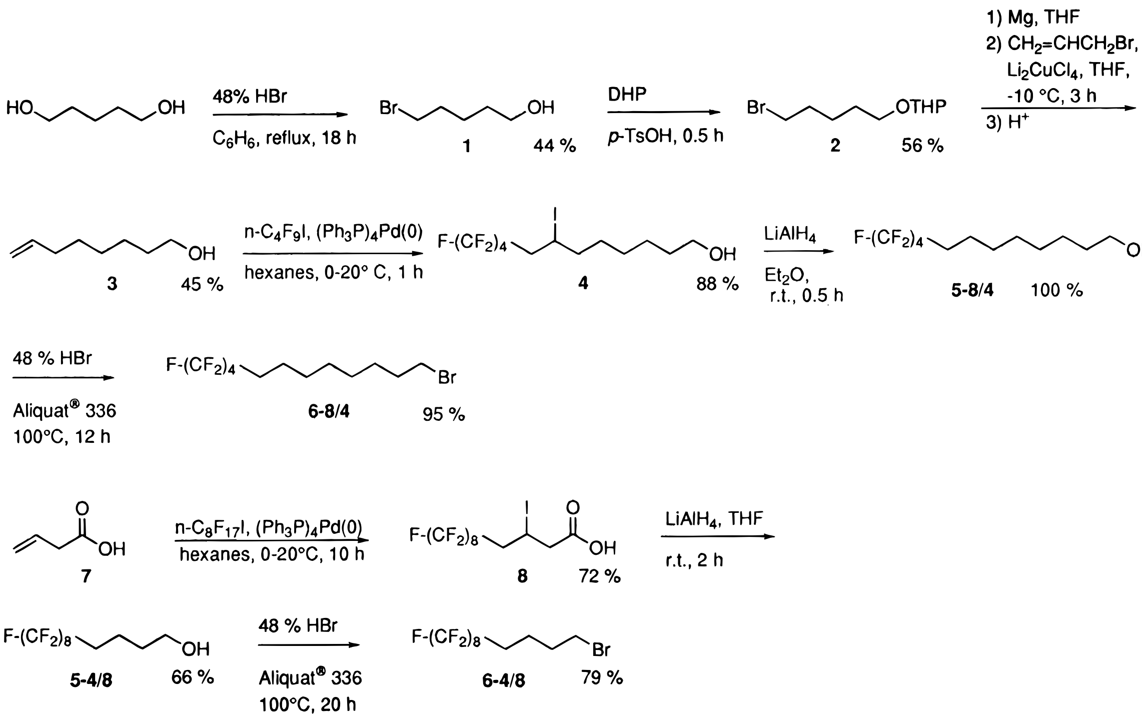

to oxygen, 4-position), 152.6 (*ipso* to oxygen, 3,5-position), 166.1 (CO_2).

2-{2-[2-(2-(Methacryloyloxy)ethoxy)ethoxy]ethoxy}ethyl 3,4,5-Tris(1*H*,1*H*,2*H*,2*H*,3*H*,3*H*,4*H*,4*H*-perfluorododecan-1-yloxy)benzoate (20-4/8). Compound **20-4/8** was synthesized according to the general procedure described for the synthesis of **20-8/4**. From **19-4/8** (0.70 g, 0.40 mmol), Et_3N (0.24 g, 2.4 mmol), and methacryloyl chloride (0.13 g, 1.2 mmol) was obtained 0.40 g (54%) of a clear oil (flash chromatography; SiO_2, 2:1 hexanes/ethyl acetate). Purity (HPLC), 99+%; TLC (2:1 hexanes/ethyl acetate), $R_f = 0.35$. ^1H NMR: 1.84−1.94 (overlapped peaks, 15H, $CF_2CH_2(C\mathit{H}_2)_2$ and CH_2=$C(C\mathit{H}_3)$), 2.16 (m, 6H, $CF_2C\mathit{H}_2$), 3.64−3.68 (overlapped peaks, 10H, CH_2=$C(CH_3)CO_2CH_2C\mathit{H}_2(OC\mathit{H}_2C\mathit{H}_2)_2$), 3.73 (t, 2H, $ArCO_2CH_2C\mathit{H}_2$, $J = 5.0$ Hz), 4.07 (overlapped t, 6H, $C\mathit{H}_2OAr$), 4.29 (t, 2H, CH_2=$C(CH_3)CO_2C\mathit{H}_2$, $J = 5.1$ Hz), 4.47 (t, 2H, $ArCO_2C\mathit{H}_2$, $J = 5.1$ Hz), 5.57 (s, 1H, $C\mathit{H}_2$=$C(CH_3)$, *trans* to C=O), 6.12 (s, 1H, $C\mathit{H}_2$=$C(CH_3)$, *cis* to C=O), 7.29 (s, 2H, *ortho* to CO_2); ^{19}F NMR: −81.5 (m, 9F, $C\mathit{F}_3$), −115.2 (m, 6F, $C\mathit{F}_2CH_2$), −122.6 (m, 18F, $(C\mathit{F}_2)_3CF_2CH_2$), −123.5 (m, 6F, $CF_3(CF_2)_2C\mathit{F}_2$), −124.1 (s, 6F, $CF_3CF_2C\mathit{F}_2$), −126.8 (m, 6F, $CF_3C\mathit{F}_2$); ^{13}C NMR: 17.1 ($CF_2CH_2\mathit{C}H_2$, 4-position), 17.3 ($CF_2CH_2\mathit{C}H_2$, 3,5-position), 18.1 (CH_2=$C(\mathit{C}H_3)$), 28.7 ($\mathit{C}H_2CH_2OAr$, 3,5-position), 29.7 ($\mathit{C}H_2CH_2OAr$, 4-position), 30.6 (t, $CF_2\mathit{C}H_2$, $J = 22.0$ Hz), 63.8 (CH_2=$C(CH_3)CO_2\mathit{C}H_2$), 64.1 ($CO_2\mathit{C}H_2$), 68.5 ($\mathit{C}H_2OAr$, 3,5-position), 69.1−70.6 ($\mathit{C}H_2O(\mathit{C}H_2\mathit{C}H_2O)_3\mathit{C}H_2$), 72.6 ($\mathit{C}H_2OAr$, 4-position), 108.2 (*ortho* to CO_2), 125.2 (*ipso* to CO_2), 125.5 ($\mathit{C}H_2$=$C(CH_3)$), 136.2 (CH_2=$\mathit{C}(CH_3)$), 142.0 (*ipso* to oxygen, 4-position), 152.5 (*ipso* to oxygen, 3,5-position), 166.1 ($Ar\mathit{C}O_2$), 167.3 (CH_2=$C(CH_3)\mathit{C}O_2$).

Polymerization of 20-m/n. All polymerizations were carried out as described below for **20-8/4**. In a flame-dried Schlenk tube equipped with a magnetic stirrer and rubber septum were added **20-8/4** (0.40 g, 0.36 mmol) and AIBN (0.59 mg, 1.0 mol %) in 0.8 mL of freshly distilled benzene. The solution was degassed with four freeze−pump−thaw cycles and then stirred at 60 °C for 20−30 h. The polymer was purified by precipitation from $CHCl_3$ or Freon 113 into hexanes. A turbid oil (0.26 g, 65%) was obtained after drying under high vacuum. The absence of monomer in the purified polymer was verified by ^1H NMR and GPC analysis. The polymer yields, molecular weights, and molecular weight distributions are summarized in Table 2.

Results and Discussion

Synthesis of Model Compounds and of Polymers. The selection of the experiments described in this publication is based on the fact that the synthesis of 3,4,5-tris(*n*-dodecan-1-yloxy)benzoic acid (**11-12/0**), 2-{2-[2-(2-hydroxyethoxy)ethoxy]ethoxy} ethyl 3,4,5-tris(*n*-dodecan-1-yloxy)benzoate (**19-12/0**), of the corresponding methacrylate (**20-12/0**) and polymethacrylate (**21-12/0**) is straightforward. In addition, all compounds are obtained in high yield and their self-assembly was investigated in detail.[1e] Finally, this tapered group represents the simplest of all the tapered componds synthesized and investigated in our laboratory.[1]

The first step in the sequence of reactions for the preparation of the corresponding compounds with semifluorinated *n*-dodecan-1-yloxy tails consists of the synthesis of the semifluorinated 3,4,5-tris(*n*-dodecan-1-yloxy)benzoic acid (**11-m/n**, where **m** + **n** = 12, **m** = number of hydrogenated methylenic groups, and **n** = number of perfluorinated methylenic groups). Two general synthetic procedures were elaborated for the preparation of **11-m/n**. The first one required the synthesis of the corresponding semifluorinated alkyl bromide (**6-m/n**) (Scheme 1) followed by alkylation of methyl 3,4,5-trihydroxybenzoate (**9**) and subsequent hydrolysis to **11-m/n** (Scheme 2). The second one consisted of the alkylation of methyl 3,4,5-trihydroxybenzoate (**9**) with a bromoalkene followed by functionalization of the vinyl groups with the perfluoroalkane segment (Scheme 3). Both reaction pathways present a series of advantages and disadvantages which will be briefly described here.

Scheme 1 outlines the synthetic methods elaborated for the preparation of **6-8/4** and **6-4/8**. They are based on the use of the most accessible and inexpensive starting materials and can be adapted without difficulty to the preparation of other functional semifluorinated compounds. The key step is the $(Ph_3P)_4Pd(0)$ catalyzed radical addition of a perfluoroalkyl iodide to a functional olefin.[20] This reaction can be carried out under ex-

Scheme 2. Synthesis of 11-m/n

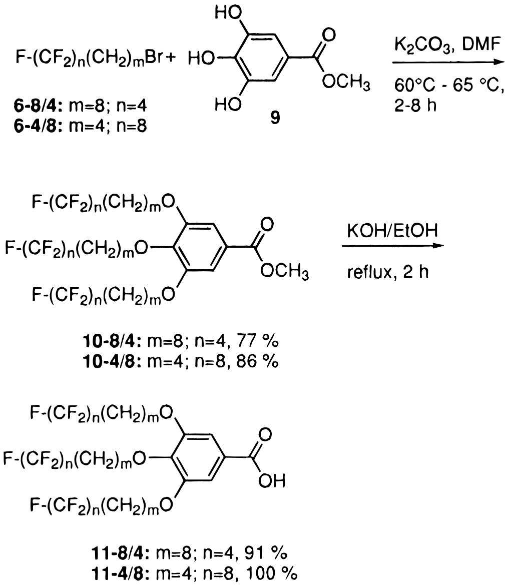

tremely mild conditions, gives high yields in short reaction times, and tolerates a large variety of functional groups. We prefer this method rather than the conventional method based on the radical addition initiated by traditional radical initiators such as peroxides or azo compounds.[7,8,26] This method requires high reaction temperatures, long reaction times, is less selective, and does not tolerate a large variety of functionalities. 7-Octen-1-ol (**3**) was synthesized by Li_2CuCl_4[10] catalyzed cross-coupling of the organomagnesium derivative of 1-bromo-5-(2-tetrahydropyranyloxy)pentane (**2**) with allyl bromide in 45% yield. Compound **2** was obtained by the monobromination of 1,5-pentanediol with HBr[16] followed by protection of the hydroxyl group of the resulted 5-bromopentan-1-ol with DHP.[18] $(Ph_3P)_4Pd(0)$ catalyzed radical addition of perfluorobutyl iodide to **3** yielded, after 1 h at room temperature, compound **4** in 88% isolated yield. The reduction of the iodo group of **4** was carried out with $LiAlH_4$ to produce **5-8/4** (100% yield). Compound **5-8/4** was brominated with HBr in the presence of Aliquat 336 as phase transfer catalyst to yield **6-8/4** in 95% yield. This method was used since previously it resulted in a 2−3-fold rate enhancement for other substrates.[22]

Compound **6-4/8** was prepared by the Pd(0) catalyzed radical addition of *n*-perfluorooctyl iodide to vinylacetic acid (**7**) to yield **8** in 72% yield. Reduction of the iodo and carboxylic groups of **8** was carried out in one step with $LiAlH_4$ to yield **5-4/8** in 66% yield. Phase transfer catalyzed bromination of **5-4/8** with HBr produced **6-4/8** in 79% yield after purification by sublimation. Although other synthetic steps were considered for the preparation of **6-8/4** and **6-4/8**, we found the procedures outlined in Scheme 1 to be both the most convenient and the least expensive. Alkylation of methyl 3,4,5-trihydroxybenzoate (**9**) with **6-8/4** and **6-4/8** in DMF at 60 °C with K_2CO_3 as base yielded after 8 h **10-8/4** in 77% and **10-4/8** in 86% yields (Scheme 2). Hydrolysis of the methyl ester group of **10-m/n** with KOH/EtOH at reflux produced **11-8/4** and **11-4/8**.

Scheme 3 outlines the second synthetic route which was used in the preparation of **11-m/n**. This procedure was applied to the synthesis of **11-6/6**. Methyl 3,4,5-trihydroxybenzoate was alkylated with 1-bromohex-5-ene (**13**) to yield **14** in 82% yield. Compound **13** was conveniently obtained by the monoelimination of HBr from 1,6-dibromohexane in HMPA.[24] Radical addition of *n*-perfluorohexyl iodide catalyzed by $(Ph_3P)_4Pd(0)$ to the double bonds of **14** yielded **15** in 80% yield. The reduction of the iodo groups was carried out with $n\text{-}Bu_3SnH$/AIBN[26] to yield **10-6/6** (complete conversion) which was hydrolyzed to **11-6/6** (56% yield from **15**) without further purification.

The advantage of the sequence of reactions from Scheme 3 is that it has fewer steps than the combination of procedures from Schemes 1 and 2, and this is advantageous if the semifluorinated **5-m/n** and/or **6-m/n** are not required for other synthetic purposes. A closer inspection of Scheme 3 would seem to indicate that all compounds, **11-m/n**, should be readily accessible from alkylation of methyl 3,4,5-trihydroxybenzoate (**9**) with appropriate 1-bromoalk-ω-enes. 1-Bromobut-3-ene was easily prepared by the monoelimination of 1,4-dibromobutane in HMPA.[24] However, an attempt to alkylate **9** with 1-bromobut-3-ene in DMF with K_2CO_3 as base resulted in the further elimination of the olefin to butadiene, so this approach was abandoned. At the same time, the monoelimination of HBr from α,ω-dibromoalkanes in HMPA relies on the ability to distill the monoeliminated product from the reaction mixture with the same rate as it is formed. Otherwise, dielimination occurs. Therefore, bromoalkenes cannot be prepared by this method from α,ω-dibromoalkanes with more than six methylenic units due to their high boiling points. For this reason, the pathway described in Schemes 1 and 2 was chosen for the synthesis of **11-4/8**.

A further limitation of the reaction Scheme 3 is that it requires the use of $n\text{-}Bu_3SnH$ in the reduction of the iodo group. Sn based side products resulted from this step are difficult to remove from the final product unless it can be recrystallized from methanol or ethanol. Alternative reduction methods using Zn/HCl[28] or SmI_2[29] resulted in a significant amount of elimination as a side reaction. The synthesis of the intermediary compounds **6-4/8** and **6-8/4** uses $LiAlH_4$ in the reduction step, and the workup of this reduction is less tedious.

The synthesis of compounds **19-8/4** was performed by the esterification of the acid chloride of **11-8/4** with the monoallyl ether of tetraethylene glycol (**16**),[14] followed by the cleavage of the allyl ether of **18-8/4** with *p*-TsOH in the presence of Pd on carbon[27] to yield **19-8/4** in 45% yield. The intermediary compound **18-8/4** was not characterized. Esterification of **19-8/4** with methacryloyl chloride produced the monomer **20-8/4** in 45% yield. Compound **19-6/6** was obtained in 39% yield by direct esterification of **11-6/6** with **16** in the presence of DCC/DPTS followed by deprotection of the allyl ether group of **18-6/6**. Compound **18-6/6** was not purified for analytical purposes. Compound **20-6/6** was prepared in 53% yield by the direct esterification of **11-6/6** with the monomethacrylate of tetraethylene glycol (**17**).[9] Product **19-4/8** (64% yield) was prepared by the same route as **19-6/6**. In this case it was necessary to use Freon 113 as a cosolvent with CH_2Cl_2 due to the poor solubility of **11-4/8**. Compound **20-4/8** (54% yield) was synthesized by the esterification of **19-4/8** with methacryloyl chloride.

Polymers **21-m/n** were obtained by the radical polymerization of the corresponding monomers **20-m/n** in benzene with AIBN as initiator (Scheme 5). **21-8/4** is soluble in $CHCl_3$ and THF while polymers **21-6/6** and **21-4/8** are soluble only in Freon 113. Due to their

Scheme 3. Synthesis of 11-6/6

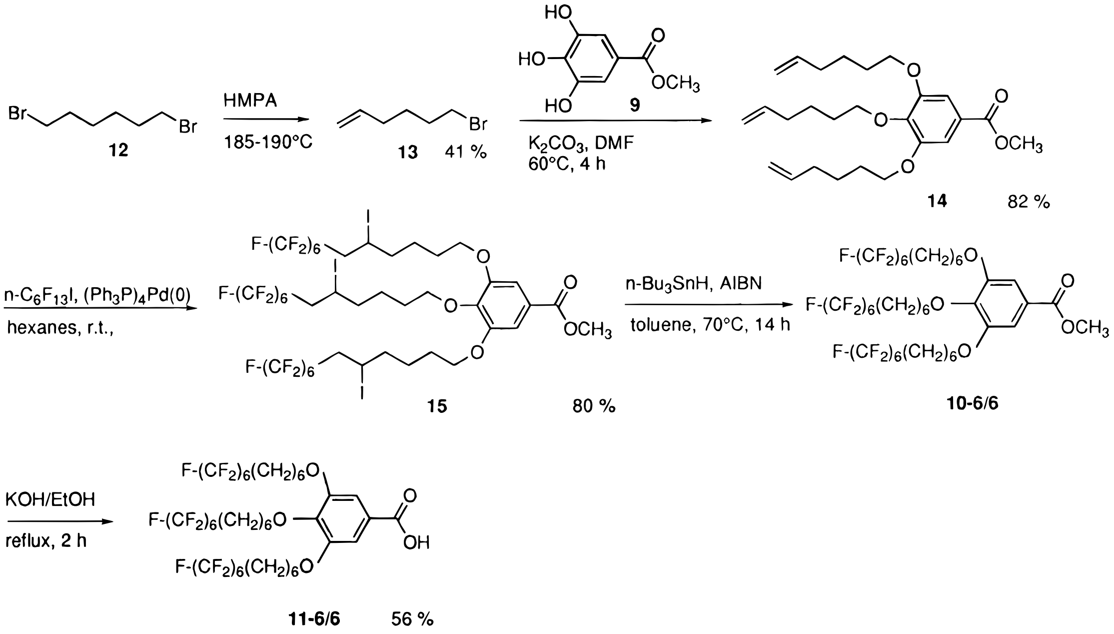

Scheme 4. Synthesis of Alcohols, 19-m/n, and Monomers, 20-m/n

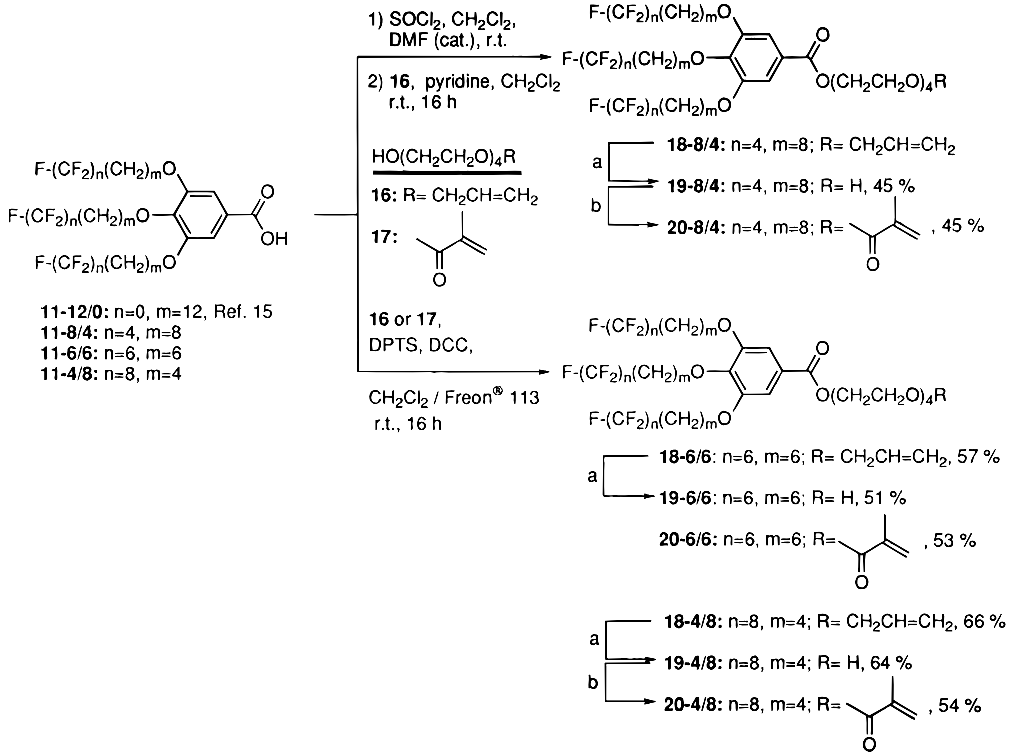

(a) 5% Pd/C, *p*-TsOH, 90 % MeOH, 100°C, 2-20 h; (b) Et$_3$N, CH$_2$=C(CH$_3$)COCl, CH$_2$Cl$_2$, 0-20°C, 2-4 h

limited solubility, the molecular weights of **21-6/6** and **21-4/8** could not be determined by GPC. These two polymers precipitate from solution during the polymerization process. The polymer yields and their molecular weight data are reported in Table 2.

Structural characterization of **11-12/0**, **19-12/0**, and **21-12/0** was reported in a previous publication[1e] and will be recapitulated briefly here (Table 1). **11-12/0** and **19-12/0** display a crystalline structure which melts directly into an isotropic liquid. Upon complexation with various alkali metal triflates, **19-12/0** self-assembles into cylindrical supramolecular structures which generate a Φ_h mesophase. The cylindrical structure of the complexes of **19-12/0** has the oligooxyethylenic segment forming the core of the cylinder and the tapered groups radiating from the center toward the periphery. In the Φ_h phase the alkyl tails of **19-12/0** are melted. The polymer, **21-12/0** generates a cylindrical structure even in the absence of complexed salts (Table 1). Most probably, a helical-like distorted conformation of the polymer backbone of **21-12/0** penetrates through the center of the column and its tapered side groups radiate toward the periphery of the column.

Thermal Characterization of Model Compounds and of Polymers. As in previous investigations,[1e] the Φ_h mesophase of all new compounds was characterized by a combination of techniques consisting of differential scanning calorimetry (DSC), X-ray diffraction, and

Scheme 5. Synthesis of Polymers, 21-m/n

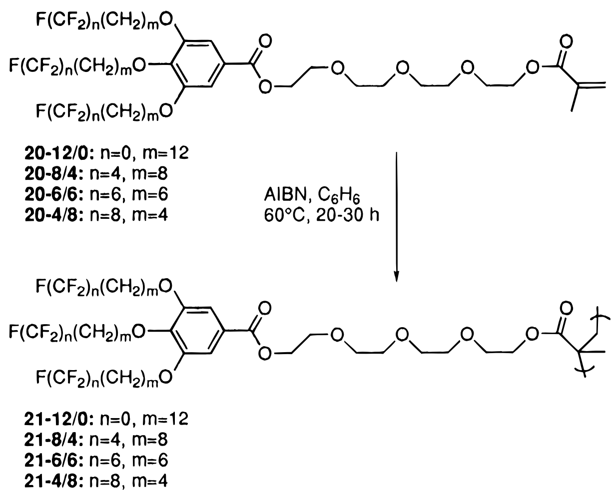

Table 1. Characterization of 11-m/n, 19-m/n, and 21-m/n[a]

	phase transitions (°C) and corresponding enthalpy changes (kcal/mol or kcal/mru)	
compd	heating	cooling
11-12/0	*k* 60 (14.9) *i* *k* 59 (14.3) *i*	*i* 33 (14.1) *k*
11-8/4	*k* −10 (3.53) Φ_h 41 (0.57) *i* *k* −11 (2.92) Φ_h 41 (0.56) *i*	*i* 35 (0.56) Φ_h −19 (2.40) *k*
11-6/6	*k* 78 (14.0[b]) Φ_h 80 (−[b]) *i* k_1 49 (4.71) k_2 76 (0.84) Φ_h 80 (0.68) *i*	*i* 73 (0.67) Φ_h 38 (4.72) *k*
11-4/8	k_1 96 (11.2) k_2 110 (7.86[b]) Φ_h 111 (−[b]) *i* k_1 100 (11.3) Φ_h 111 (1.19) *i*	*i* 108 (1.16) Φ_h 56 (1.42) k_2 35 (1.14) k_1
19-12/0	k_1 19 (0.78) k_2 30 (18.94) *i* *k* 23 (16.4) *i*	*i* 7 (16.1) *k*
19-8/4	*k* −17 (5.92) Φ_h 1 (0.24) *i* *k* −17 (5.30) Φ_h −2 (0.19) *i*	*i* −9 (0.20) Φ_h −31 (6.29) *k*
19-6/6	*k* 8 (5.78) Φ_h 31 (0.36) *i* *k* 8 (5.90) Φ_h 31 (0.19) *i*	*i* 25 (0.17) Φ_h −4 (5.51) *k*
19-4/8	*k* 35 (7.01) Φ_h 68 (0.47) *i* k_1 25 (1.01) *k* 26 (−1.34) *k* 35 (5.01) Φ_h 67 (0.32) *i*	*i* 63 (0.32) Φ_h 18 (3.43) *k*
21-12/0	*k* 17 (6.05) Φ_h 54 (0.20) *i* *k* 17 (6.53) Φ_h 54 (0.16) *i*	*i* 37 (0.23) Φ_h 3 (5.88) *k*
21-8/4	*g* −34 Φ_h 89 (0.10) *i* *g* −32 Φ_h 88 (0.15) *i*	*i* 67 (0.11) Φ_h −37 *g*
21-6/6	*g* −4 Φ_h 140[c] (−) *i* *g* −6 Φ_h 125[c] (−) *i*	*i* 125[c] (−) Φ_h −11 *g*
21-4/8	*g* 16 Φ_h 129 (0.27) *i* *g* 16 Φ_h 126 (0.22) *i*	*i* 118 (0.20) Φ_h 9 *g*

[a] Data on the first lines under heating and cooling are determined during the first heating and cooling scans. Data on the second line under heating are determined during the second heating scan. [b] Overlapped peaks. [c] Transitions determined by optical polarized microscopy.

Table 2. Characterization of Polymethacrylates 21-m/n by Size Exclusion Chromatography

polymer	polymer yield (%)	$M_w \times 10^{-3}$ [a]	$M_n \times 10^{-3}$ [a]	M_w/M_n	DP
21-12/0	47	46.0	26.7	2.67	29
21-8/4	45	61.0	50.0	1.22	35
21-6/6	49	—[b]	—[b]	—[b]	—[b]
21-4/8	26	—[b]	—[b]	—[b]	—[b]

[a] Referenced to linear polystyrene standards. [b] Polymer was insoluble in THF but soluble in Freon 113.

thermal optical polarized microscopy. We will discuss first the phase behavior of **11-m/n**, **19-m/n**, and **21-m/n** compounds based on their DSC traces. The assignment of various phases observed by DSC was done by X-ray diffraction experiments.

Figure 1 presents the first heating (a), cooling (b), and the second heating (c) DSC traces of **11-m/n**. An investigation of the first DSC scans provided the following results. **11-12/0** shows a crystalline phase which melts at 60 °C. The replacement of the four outer methylenic groups of the alkyl tails of **11-12/0** with four perfluorinated methylenic groups produces **11-8/4** which has a much lower melting temperature, i.e., at −10 °C, followed by a Φ_h phase which undergoes isotropization at 41 °C. Increasing the number of perfluorinated methylenic groups to six increases both the melting temperature to 78 °C and the isotropization temperature of the Φ_h phase of **11-6/6** to 80 °C. Our previous report which was based on a single perfluorinatred segment length[9] showed nearly identical results. In that case, the analogue of **11-12/0** derived from ten methylenic groups in the alkyl tails (**11-10/0**) is crystalline and melts at 53 °C. Replacement of the outer six methylenic groups with perfluorinated groups yielded **11-6/4**, which is crystalline and melts at 76 °C into a Φ_h phase followed by isotropization at 79 °C. The trend continues for the case of **11-4/8** (**n** = 8) which has a melting at 110 °C and an isotropization of the Φ_h phase at 111 °C. While in the first scan the melting of **11-6/6** and **11-4/8** are overlapping the isotropization of the Φ_h phase, in the second and subsequent heating scans the melting temperatures are suppressed and therefore, the Φ_h phase has a broader range of temperature than in the first heating scan.

The melting and isotropization temperatures of **11-m/n** obtained from Figure 1 and summarized in Table 1 are plotted as a function of the number of perfluorinated methylenic units, **n**, in Figure 2. The plots from Figure 2 provide the following conclusion. A very short perfluorinated segment (i.e., four perfluorinated methylenic groups out of 12) has a drastic effect on the melting temperature of **11-m/n**, lowering it by 70 °C. At the same time it increases dramatically the ability of **11-m/n** to form a Φ_h phase. As a result, while **11-12/0** does not self-assemble into a cylindrical supramolecular structure, its homologue, **11-8/4**, produces a column which generates a Φ_h phase that is stable over a range of 51 °C. This behavior is the result of two opposite effects generated by semifluorination, i.e, a decreased crystallization tendency and an increased ability to form the cylindrical self-assembly. However, at this point we are not certain if **11-12/0** does not exhibit a virtual Φ_h phase and that the effect of the small extent of fluorination is mostly to uncover th Φ_h phase by lowering the melting temperature. The effect obtained upon further increase of the length of the perfluorinated segment from four to six and eight methylenic groups respectively is very clear. It increases both the melting and the isotropization temperatures. As a consequence, since the slope of the melting temperature as a function of **n** is higher than that of the isotropization temperature, although both transition temperatures increase, the temperature range of the Φ_h phase becomes narrower (Figure 2).

The upper part of Figure 3 presents the DSC traces of **19-m/n**. The trend observed for **19-m/n** is almost similar to that observed for **11-m/n**. That is, **19-12/0** is only crystalline. Replacement of four methylenic units from the alkyl tails of **19-12/0** with semifluorinated groups produces **19-8/4**, which has a much lower melting transition and an enantiotropic Φ_h phase. Increasing the length of the semifluorinated segment

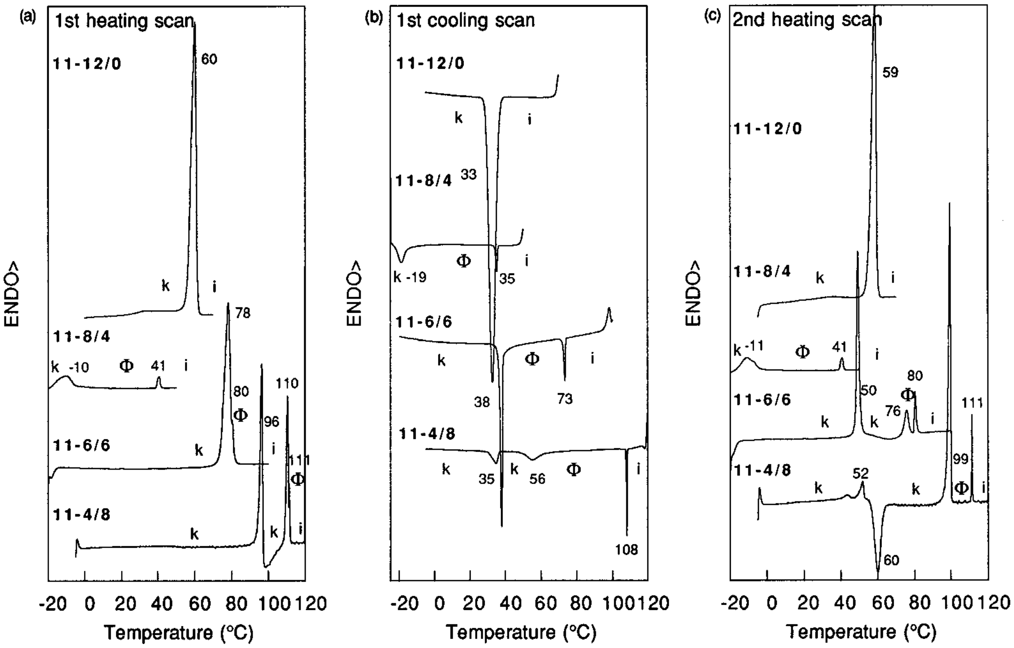

Figure 1. Representative DSC traces (10 °C min^{-1}) of **11-m/n** recorded during (a) the first heating scan; (b) the first cooling scan; and (c) the second heating scan.

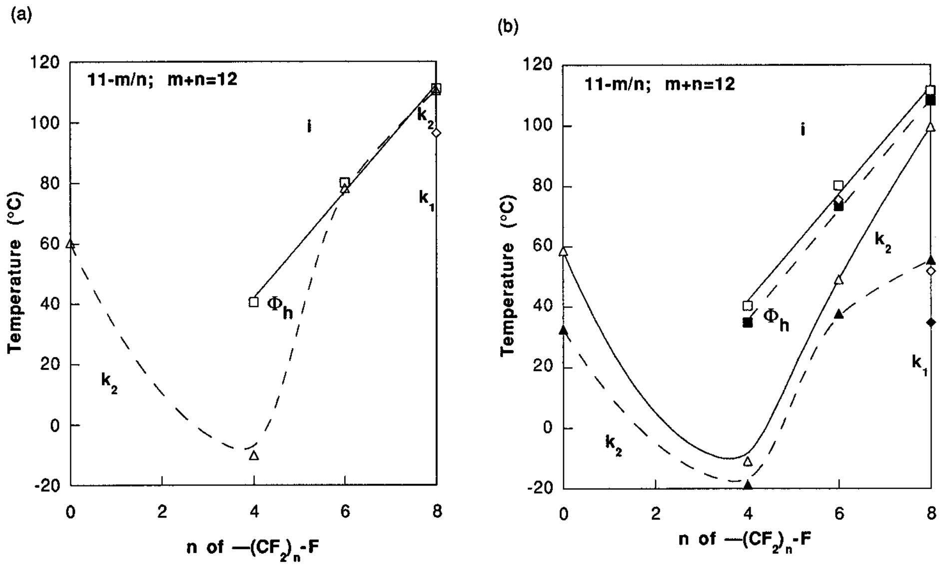

Figure 2. Dependence of the phase transitions of **11-m/n** on the number of fluorinated methylenes in the alkyl tails (*n*). (a) Data from the first heating scan are (◇) T_{m1}; (△) T_{m2}; (□) $T_{\Phi_h\text{-}i}$. (b) Data from the cooling scan are (◆) T_{k1}; (▲) T_{k2}; (■) $T_{i\text{-}\Phi_h}$. Data from the second heating scan are (◇) T_{m1}; (△) T_{m2}; (□) $T_{\Phi_h\text{-}i}$.

increases both the melting and the isotropization temperatures. This trend is even more clearly observed in Figure 4, which plots the melting and isotropization temperatures of 19-**m/n** as a function of **n**.

Finally, the bottom part of Figure 3 presents the DSC traces of the polymers **21-8/4**, **21-6/6**, and **21-4/8**. All polymers exhibit a Φ_h phase. For the case of **21-6/6**, a first order transition peak associated with the isotropization temperature was not observed in the DSC scans. However, a birefrigent texture was observed by thermal optical polarized microscopy that persisted on heating up to 140 °C. On subsequent cooling the texture of the Φ_h phase was observed at 129 °C. The isotropization temperature of the Φ_h phase increases with the increase of **n**. These polymers are not crystallizable. Their T_g values (Figure 3) follow a similar trend with their isotropization, i.e. they increase with the increase of the extent of fluorination. Figure 5 summarizes both the isotropization and the glass transition temperatures of **21-8/4**, **21-6/6**, and **21-4/8** and compares them with the same data of **21-12/0** collected from a previous publication.[1g] Since **21-12/0** also exhibits a Φ_h phase, the plot from Figure 5 demonstrates the dramatic stabilization of the Φ_h phase of **21-m/n** upon fluorination. The isotropization temperature of **21-4/8** is lower than that of **21-6/6**, most probably due to a lower molecular weight of **21-4/8**. This is due to the lower solubility of **21-4/8** in the polymerization solvent, resulting in an earlier precipitation of a lower molecular weight polymer. Table 2 summarizes the characterization of **11-m/n**, **19-m/n**, and **21-m/n**.

Figure 6 plots the dependence of the hexagonal columnar–isotropic transition temperatures ($T_{\Phi_h\text{-}i}$) as a function of the number of fluorinated methylenic groups, **n**, for all three of the systems investigated in this series of experiments. The supramolecular columns derived from **11-m/n**, **19-m/n**, and **21-m/n** are derived from the same tapered groups but differ in the func-

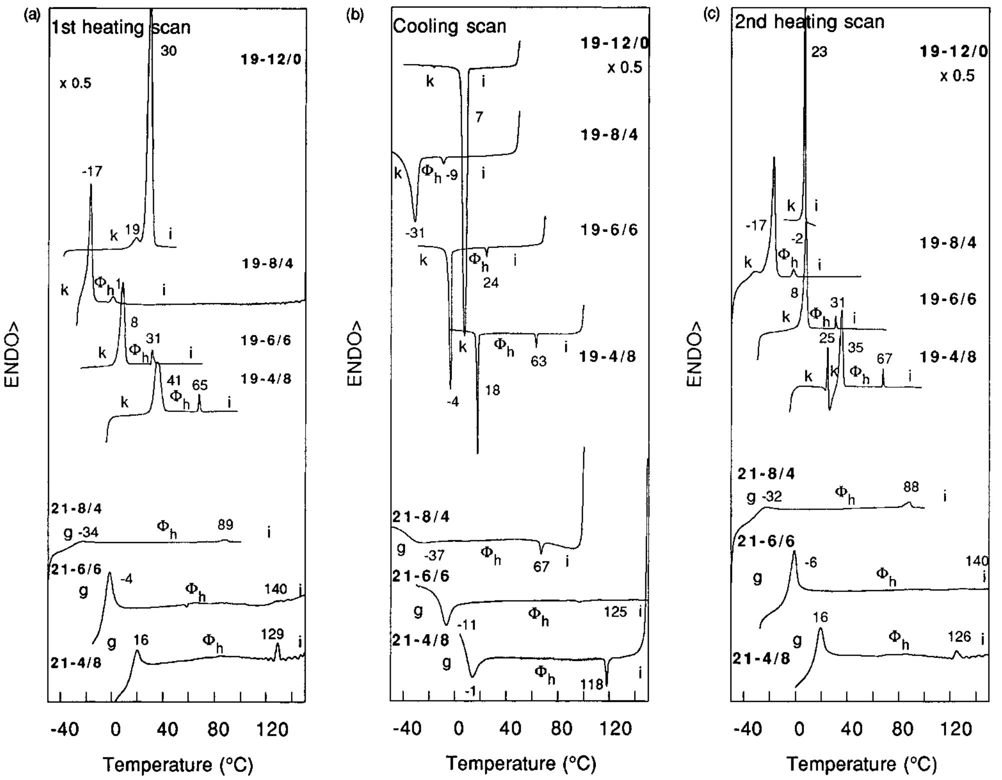

Figure 3. Representative DSC traces (10 °C min^{-1}) of **19-m/n** and **21-m/n** recorded during (a) the first heating scan; (b) the first cooling scan; and (c) the second heating scan.

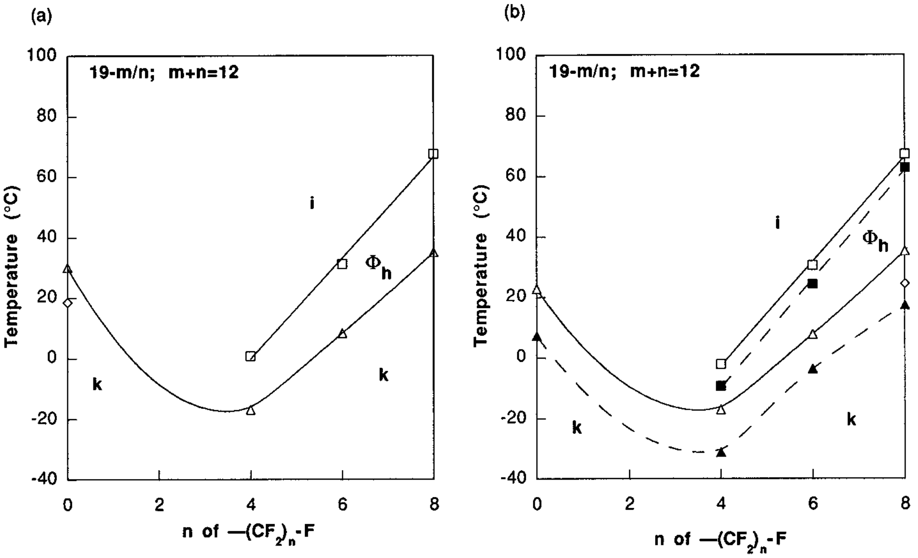

Figure 4. Dependence of the phase transitions of **19-m/n** on the number of fluorinated methylenes in the alkyl tails (n). (a) Data from the first heating scan are (△) T_m; (□) $T_{\Phi_h\text{-}i}$. (b) Data from the cooling scan are (▲) T_k; (■) $T_{i\text{-}\Phi_h}$. Data from the second heating scan are (△) T_m; (□) $T_{\Phi_h\text{-}i}$.

tionalization of their core. Specifically, **11-m/n**, **19-m/n**, and **21-m/n** are functionalized with carboxylic acid, hydroxy terminated oligooxyethylenic, and polymethacrylate terminated oligooxyethylenic functional groups, respectively. These groups play the role of the *endo*-receptor in the self-assembly and thus contribute to the overall stability of the supramolecular column and of the Φ_h phase. Inspection of Figure 6 shows that the highest $T_{\Phi_h\text{-}i}$, and thus stabilities, are observed for the series of polymers, **21-m/n**, followed by the benzoic acids, **11-m/n**, and alcohols, **19-m/n**. This order arises from the difference between stabilization of the supramolecular column by H-bonding and by covalent attachment to a backbone. **19-m/n**, having the weakest O-H- -O-H-bonding interaction has the lowest range of $T_{\Phi_h\text{-}i}$ while **11-m/n**, which have a much stronger carboxylic H-bonding interaction, exhibit higher stabilities. Finally, when H-bonding is replaced by the covalent bond of the polymethacrylate backbone of **21-m/n**, the highest isotropization temperatures are observed.

The increase in the $T_{\Phi_h\text{-}i}$ as a function of the number of fluorinated methylenic units, n, in the alkyl tails is linear ($R^2 > 0.99$) for **11-m/n** and **19-m/n**. For the case of **21-m/n**, a strict linear dependence is not observed due to the molecular weight effect which was discussed previously. However, to compare **11-m/n** and **19-m/n**, the graphical data of Figure 6 were fitted to a straight line. The slopes of these lines represent the incremental

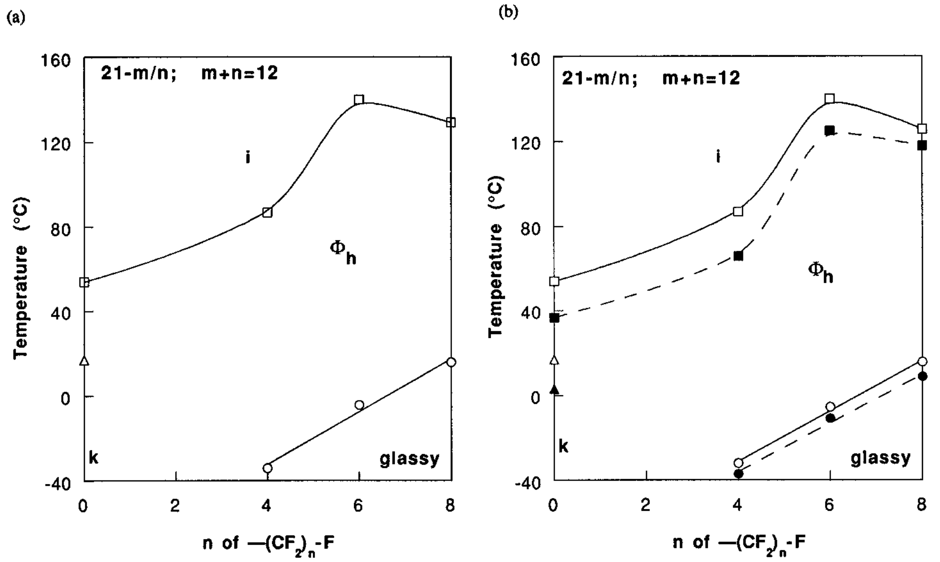

Figure 5. Dependence of the phase transitions of **21-m/n** on the number of fluorinated methylenes in the alkyl tails (*n*). (a) Data from the first heating scan are (○) T_g; (□) $T_{\Phi_h\text{-}i}$. (b) Data from the cooling scan are (●) T_g; (▲) T_k; (■) $T_{i\text{-}\Phi_h}$. Data from the second heating scan are (○) T_g; (△) T_m; (□) $T_{\Phi_h\text{-}i}$.

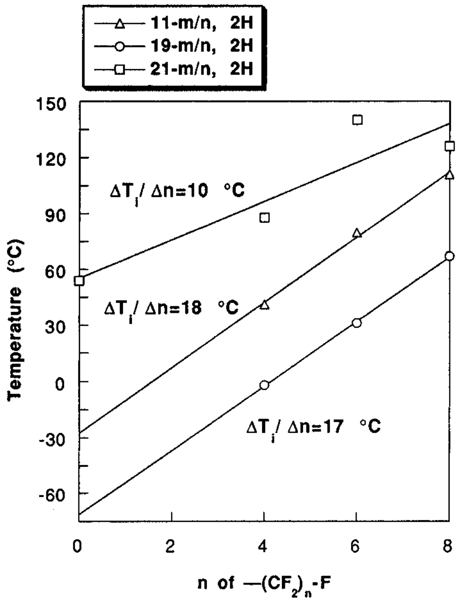

Figure 6. Dependence of the isotropization temperature ($T_{\Phi_h\text{-}i}$) of (a) (△) **11-m/n**; (b) (○) **19-m/n**; and (c) (□) **21-m/n** on the number of fluorinated methylenes in the alkyl tails (*n*). Data are from the second heating scan.

contribution of each fluorinated methylenic unit to the thermodynamic stability of the Φ_h phase and are depicted in Figure 6 as $\Delta T_i/\Delta n$. For **11-m/n** and **19-m/n**, each fluorinated methylenic unit in the alkyl tails increases the isotropization temperature by 17−18 °C. For **21-m/n**, the contribution is smaller (~10 °C) but still significant. The overall consequence is that a dramatic stabilization of the Φ_h phase is observed upon fluorination, more so than the effect of H-bonding or covalent attachment to a polymeric backbone. For example, **19-12/0** does not exhibit a Φ_h mesophase. However, upon covalent attachment to a polymeric backbone as exemplified by **21-12/0**, it exhibits an enantiotropic Φ_h mesophase that undergoes isotropization at 54 °C. If eight of the twelve methylenic units of **19-12/0** are perfluorinated as exemplified by **19-4/8**, an enantiotropic Φ_h mesophase that undergoes isotropization at 67 °C is obtained. This represents a 13 °C increase in the mesophase stability over that of the perhydrogenated polymer **21-12/0**. Similar comparisons can be made for **11-m/n** as well.

Figure 7a plots the molar transition enthalpies ($\Delta H_{\Phi_h\text{-}i}$) (Table 1) for **11-m/n**, **19-m/n**, and **21-m/n** as a function of **n**. The same data are plotted in Figure 7b for the molar transition entropies ($\Delta S_{\Phi_h\text{-}i}$). Both $\Delta H_{\Phi_h\text{-}i}$ and $\Delta S_{\Phi_h\text{-}i}$ are small and characteristic of Φ_h-i transitions.[1] As the extent of fluorination increases, the corresponding $\Delta H_{\Phi_h\text{-}i}$ and $\Delta S_{\Phi_h\text{-}i}$ increase for **11-m/n**, **19-m/n**, and **21-m/n**. Since $T_{\Phi_h\text{-}i} = \Delta H_{\Phi_h\text{-}i}/\Delta S_{\Phi_h\text{-}i}$, an increase in isotropization temperature results from the greater increase in $\Delta H_{\Phi_h\text{-}i}$ relative to $\Delta S_{\Phi_h\text{-}i}$.

Characterization by X-ray Diffraction Experiments. Table 3 summarizes the characterization of the Φ_h phase of **11-m/n**, **19-m/n**, and **21-m/n** by X-ray diffraction experiments. Details on the interpretation of the X-ray data for Φ_h phases were presented in previous publications.[1a−e] The Φ_h phase is characterized by the presence of three X-ray reflections in the small angle range, with spacings in the ratio d_{100}:d_{110}:$d_{200} = 1:(1/\sqrt{3}):(1/2)$. Only diffuse scattering is observed at wide angles. The measured small-angle spacings are summarized in Table 3. The hexagonal lattice parameter ($a = \langle d_{100}^{\text{hex}}\rangle/\sqrt{3}$) is equal to the diameter of the self-assembled columns which are responsible for the generation of the Φ_h phase. Figure 8 plots the diameter of these columns as a function of **n** for **11-m/n**, **19-m/n**, and **21-m/n**. This figure indicates the following general trend. When only four methylenic groups are perfluorinated, the diameter of the self-assembled column does not change from that of the column obtained with non-fluorinated tails. However, a subsequent increase of the number of perfluorinated methylenic groups, from four to six and respectively eight, enlarges the column diameter.

Figure 9 displays the unminimized molecular structures of (a) **21-12/0** and (b) **21-4/8**. The alkyl tails are presented in the lowest energy *all-trans* configuration, and they are planar with respect to the benzene ring. The oligooxyethylenic segment is also drawn in the *all-trans* extended conformation. A 7_2 helical conformation of the oligooxyethylenic segment is more stable,[3] but for purposes of comparison, the *all-trans* conformation is depicted here. The end-to-end molecular distances are

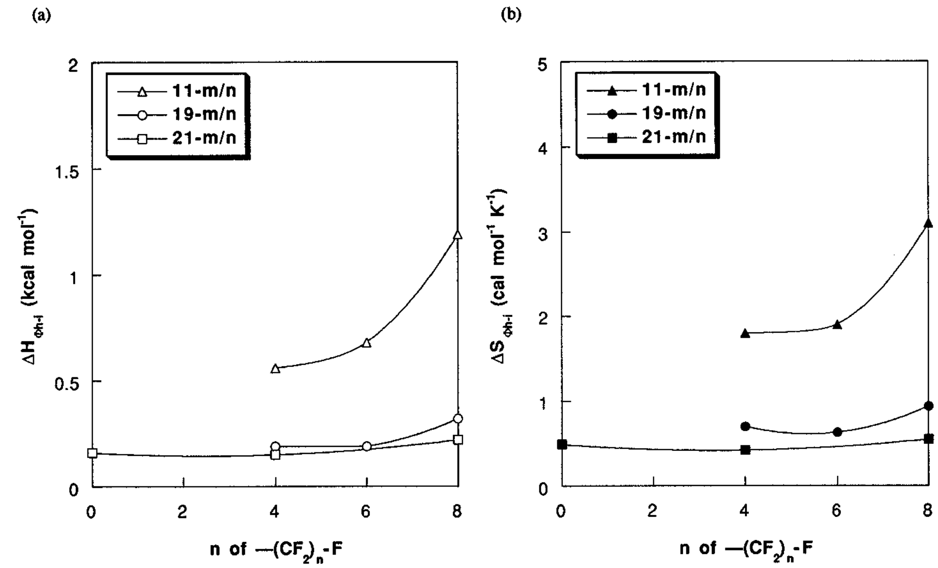

Figure 7. (a) Dependence of the enthalpy change ($\Delta H_{\Phi_h\text{-}i}$) on isotropization of **11-m/n** (△), **19-m/n** (○), and **21-m/n** (□) on the number of fluorinated methylenes in the alkyl tails (*n*). Data are from the second heating scan. (b) The dependence of the entropy change ($\Delta S_{\Phi_h\text{-}i}$) on isotropization of **11-m/n** (▲), **19-m/n** (●), and **21-m/n** (■) on the number of fluorinated methylenes in the alkyl tails (*n*). Data are from the second heating scan.

Table 3. Characterization of the Φ_h Phase of 11-m/n, 19-m/n, and 21-m/n by Small Angle X-ray Scattering

compd	*n*	*T* (°C)	d_{100}^{hex} (Å)	d_{110}^{hex} (Å)	d_{200}^{hex} (Å)	d_{210}^{hex} (Å)	$\langle d_{110}^{\mathrm{hex}}\rangle^a$ (Å)	a^b (Å)	R^c (Å)	S^d (Å)
11-12/0	0									
11-8/4	4	30	29.1	16.6	14.6		29.0	33.5	16.8	19.3
11-6/6	6	73	29.1	16.3	14.4		28.7	33.2	16.6	19.1
11-4/8	8	75	31.6	18.1		11.8	31.5	36.3	18.2	21.0
19-12/0	0									
19-8/4	4									
19-6/6	6	29	39.2	22.6	19.7		39.2	45.3	22.7	26.2
19-4/8	8	29					40.5	46.8	23.4	27.0
	8	50	38.4	22.6	19.6		38.9	44.9	22.5	25.9
21-12/0	0	27	42.1	24.2	21.1	15.7	42.1	48.6	24.3	28.0
	0	41	40.8	23.6	20.6	15.4	41.0	47.3	23.6	27.3
21-8/4	4	30	41.8	24.0	21.0		41.8	48.3	24.1	27.9
21-6/6	6	28	43.0	25.1	21.9		43.3	50.1	25.1	29.0
21-4/8	8	28	47.2		23.6	18.0	47.2	54.5	27.3	31.5

[a] $\langle d_{100}^{\mathrm{hex}}\rangle = [d_{100}^{\mathrm{hex}} + (d_{110}^{\mathrm{hex}} \times \sqrt{3}) + (d_{200}^{\mathrm{hex}} \times 2)]/3$. [b] $a = 2\langle d_{100}^{\mathrm{hex}}\rangle/\sqrt{3}$. [c] $R = \langle d_{100}^{\mathrm{hex}}\rangle/\sqrt{3}$. [d] $S = 2R/\sqrt{3}$.

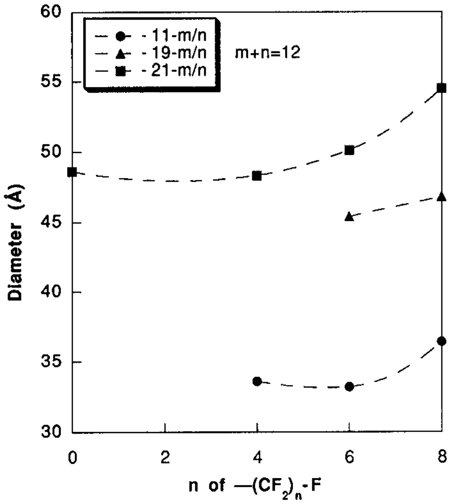

Figure 8. Dependence of the column diameter, *a*, of (●) **11-m/n**, (▲) **19-m/n**, and (■) **21-m/n** on the number of fluorinated methylenes in the alkyl tails (*n*).

indicated for (a) **11-12/0**, **19-12/0**, and **21-12/0** and (b) **11-4/8**, **19-4/8**, and **21-4/8**. The end-to-end molecular distance of **11-4/8** is 0.7 Å longer than the same distance from **11-12/0**. This increase is due to the the longer-CF_2CF_2-bond length (1.58 Å) compared to the -CH_2CH_2-bond length (1.54 Å). The increased bond length is not sufficient to account for the 2−3 Å increase in the column diameter with fluorination. Other factors, such as the increased rigidity of the perfluoroalkane segments may contribute as well. Further analysis of Figure 8 shows that the column diameter of the self-assembled structures increases in the order **21-m/n** > **19-m/n** > **11-m/n**. Inspection of Figure 9 shows that this is clearly a result of the increase of the end-to-end molecular distance on the sequential addition of oligooxyethylenic and methacrylate moieties, respectively, and this result is in agreement with previous data reported from our laboratory.[1c−e]

Self-Assembly Mechanism. Figure 10 presents a schematic representation of the self-assembly of semifluorinated tapered groups into a supramolecular column which generates a Φ_h mesophase. This scheme is based on previous examples of self-assembly of nonfluorinated[1−3] and fluorinated[9] tapered groups from our laboratory. The tapered groups, **11-m/n** and **19-m/n**, self-assemble into a supramolecular disc-like unit. The entropy loss during this process is compensated by the exoenthalpic process generated by H-bonding. These discs can then stack into a supramolecular columnar architecture which minimizes the free energy of the system due to packing into a Φ_h phase. The “hydrophilic” oligooxyethylenic segment resides within the center of the column and in the case of **21-m/n**, the backbone penetrates this matrix. We envision some distortion of the polymer backbone, possibly helical, due to organization of the tapered side groups.[3] The aromatic moieties form a rigid core that stabilizes the structure. Their orientation with respect to the columnar axis is not clear, but X-ray experiments suggest that they are somewhat tilted.[3] By analogy with low molar mass and polymeric liquid crystals formed from discotic mesogens, the alkyl tails of this system are melted. This is supported by the fact that the lattice parameter, *a*, observed by X-ray diffraction experiments is significantly smaller than the lattice parameter expected from

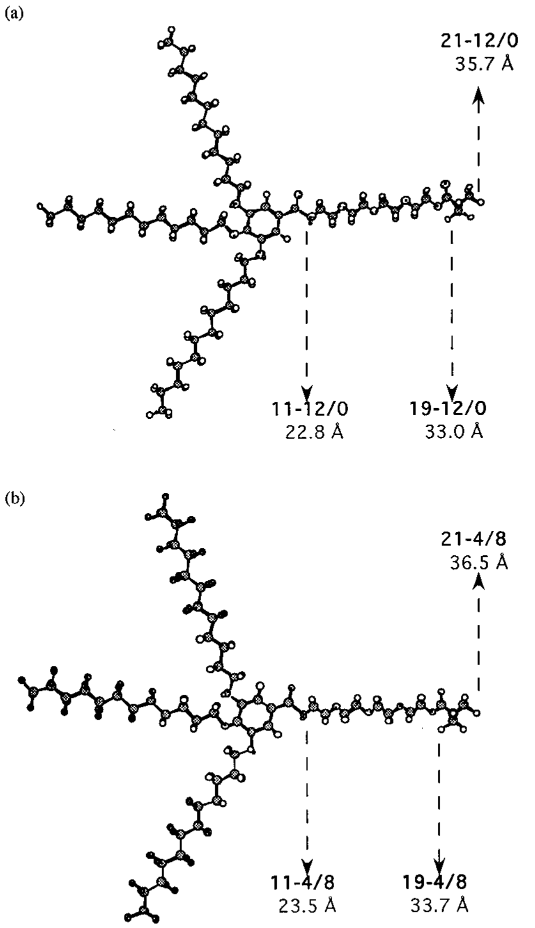

Figure 9. Unminimized molecular model of (a) **21-12/0** and (b) **21-4/8**.

a columnar structure in which the alkyl tails exist in the *all-trans* conformation.[1] However, at a certain ratio, the perfluorinated segments are expected to be microphase segregated from the perhydrogenated segments due to their mutual incompatibility.[30] As a consequence, these tubular architectures should have fluorine enriched, low energy surfaces. The supramolecular columns stack into a hexagonal lattice. This hexagonal lattice should have periodic fluctuations in composition between oligooxyethylenic, hydrocarbon, and fluorocarbon blocks as depicted in Figure 10.

From the experimental results generated by this research we can speculate that the dramatically enhanced ability of **11-m/n**, **19-m/n**, and **21-m/n** to self-assemble upon semi-fluorination arises from a combination of two competitive and two cooperative effects which are generated by the fluorophobic effect. These two sets of effects can be discussed by inspecting once again Figures 2, 4, and 5. Increasing **n** from 0 to 4 decreases the melting temperature of **11-12/0** and **19-12/0** (Figures 2 and 4). No information about the change of **n** from 0 to 4 on the isotropization transition of the Φ_h phase is available from these two sets of data. However, after inspection of Figure 5, we can see that the isotropization of the Φ_h phase of **21-12/0** increases by 35 °C from **n** = 0 to **n** = 4, i.e., for the case of **21-8/4**. Therefore, we can assume that a similar effect may occur in the case of **11-12/0** and **19-12/0**. The potential "virtual"[31] Φ_h phase of **11-12/0** and **19-12/0** increases its isotropization transition temperature. As a result of these two opposite trends, **11-8/4** and **19-8/4** exhibit an enantiotropic Φ_h phase. A further increase in **n** from 4 to 6 and 8 increases both the melting and isotropization transition temperatures (Figures 2 and 4). Depending on the relative slopes of these two dependences on **n** at values of **n** larger than 4, the range of the Φ_h phase becomes broader or narrower. Therefore, the fluorophobic effect is determined by the "eutectic-like" phase diagram of the crystalline phase and probably ideal solution-like phase (continuous dependence of $T_{\Phi_h\text{-}i}$ vs **n**) behavior of the Φ_h phase of **11-m/n** and **19-m/n** as a function of **n**. The net effect of this combination is the dramatically enhanced ability of these tapered groups to self-assemble into supramolecular columns. The eutectic behavior of the crystalline phase is due to the decreased melting of the parrafinic segment by the fluorinated one at **n** = 4 and decreased melting of the fluorinated segment by the parrafinic segment at **m** = 4 and 6. The immiscibility in the melt phase of the outer layer of the supramolecular columns (Figure 10) can explain the continuous increase in $T_{\Phi_h\text{-}i}$ and column diameter with increasing **n**. It has been demonstrated that columnar architectures derived from tapered groups containing ((*n*-alkyloxy)benzyl)oxy tails exhibit greater

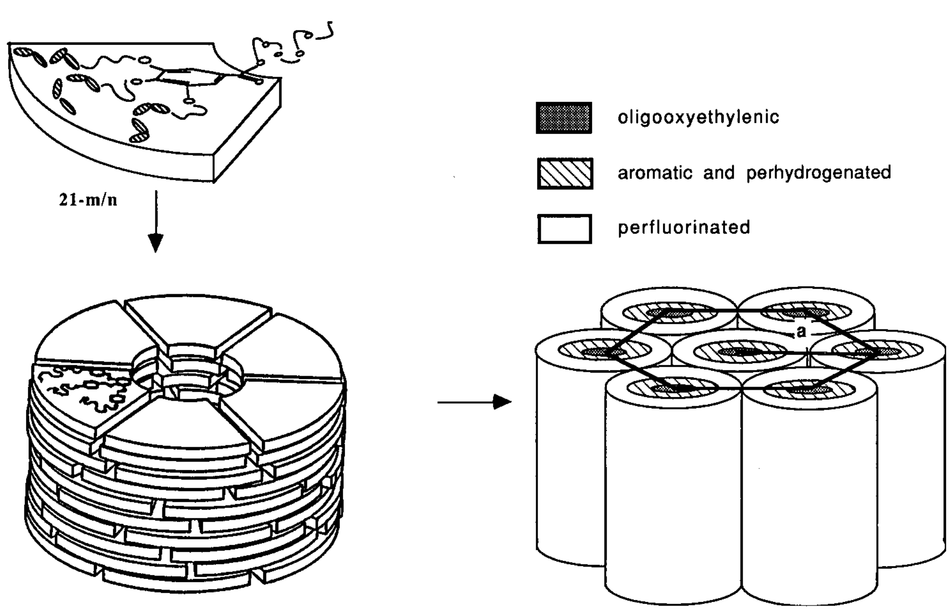

Figure 10. Schematic representation of the self-assembly of **21-m/n** into a tubular supramolecular architecture.

thermodynamic stabilities of their Φ_h phase than those based on their *n*-alkyloxy analogues.[1d–g] The wider and more rigid tapered group in the former stabilizes the cylindrical assembly. Fluoroalkanes have a van der Waals cross-sectional area of 28.3 Å^2 while the same dimension for *all-trans* planar zig zag alkanes is 18.5 Å^2.[4] Thus in the melted phase of the microsegregated tapered group, an increased cross-sectional area due to the presence of the perfluoroalkyl segment contributes to the formation of a wider tapered group which subsequently induces a greater mesophase stability. Additional increase is due to the higher rigidity[4c] of the perfluorinated segments and the high enthalpy of mixing of perfluorinated and perhydrogenated segments. The microsegregation of the perfluorinated and perhydrogenated outer layer of the supramolecular column provides a lower degree of packing which favors a more extended chain length in each phase and, therefore, a larger column diameter. Additional experiments required to elucidate the self-assembly mechanism *via* the fluorophobic effect are in progress.

The results presented in this publication are very rewarding since tapered groups such as those described in this and other publications from our[1–3,9,32] and other laboratories[33] are extensively used in the design and self-assembly of new molecular, macromolecular, and supramolecular architectures. The enhanced ability to self-assemble tapered groups *via* the fluorophobic effect provides new synthetic strategies in these fields.

Acknowledgment. Financial support by the National Science Foundation (DMR 92-06781), IBM and Sicka Graduate Fellowships (to G.J.), the Engineering and Physical Science Research Council, U.K., and NATO (traveling grant) is gratefully acknowledged.

References and Notes

(1) For selected publications on the self-assembly of taper shaped groups and of their polymers, see: (a) Percec, V.; Johansson, G.; Heck, J.; Ungar, G.; Batty, S. V. *J. Chem. Soc., Perkin Trans. 1* **1993**, 1411. (b) Johansson, G.; Percec, V.; Ungar, G.; Abramic, D. *J. Chem. Soc., Perkin Trans. 1* **1994**, 447. (c) Percec, V.; Heck, J.; Tomazos, D.; Falkenberg, F.; Blackwell, H.; Ungar, G. *J. Chem. Soc., Perkin Trans. 1* **1993**, 2799. (d) Percec, V.; Heck, J.; Tomazos, D.; Ungar, G. *J. Chem. Soc., Perkin Trans. 2* **1993**, 2381. (e) Percec, V.; Tomazos, D.; Heck, J.; Blackwell, H.; Ungar, G. *J. Chem. Soc., Perkin Trans. 2* **1994**, 31.

(2) For some recent reviews on the self-assembly of taper shaped groups, see: (a) Percec, V.; Heck, J.; Johansson, G.; Tomazos, D.; Ungar, G. *Macromol. Symp.* **1994**, *77*, 237. (b) Percec, V.; Heck, J.; Johansson, G.; Tomazos, D.; Kawasumi, M.; Chu, P.; Ungar, G. *J. Macromol. Sci.—Pure Appl. Chem.* **1994**, *A31*, 1719. (c) Percec, V.; Heck, J.; Johansson, G.; Tomazos, D.; Kawasumi, M.; Chu, P.; Ungar, G. *Mol. Cryst. Liq. Cryst.* **1994**, *254*, 137.

(3) For publications on the structural characterization of the supramolecular tubular architectures self-assembled from tapered building blocks, see: (a) Kwon, Y. K.; Chvalun, S.; Schneider, A.-I.; Blackwell, J.; Percec, V.; Heck, J. A. *Macromolecules* **1994**, *27*, 6129. (b) Kwon, Y. K.; Danko, C.; Chvalun, S.; Blackwell, J.; Heck, J.; Percec, V. *Macromol. Symp.* **1994**, *87*, 103. (c) Kwon, Y. K.; Chvalun, S. N.; Blackwell, J.; Percec, V.; Heck, J. A. *Macromolecules* **1995**, *28*, 1552.

(4) (a) Smart, B. E. In *Organofluorine Chemistry. Principles and Commercial Applications*; Banks, R. E., Smart, B. E., Tatlow, J. C., Eds.; Plenum: New York, 1994, p 57. (b) Feiring, A. E. *J. Macromol. Sci.—Pure Appl. Chem.* **1994**, *A31*, 1657. (c) Eaton, D. F.; Smart, B. E. *J. Am. Chem. Soc.* **1990**, *112*, 2821.

(5) For examples on the stabilization of thermotropic mesophases by replacing perhydrogenated with perfluorinated segments: (a) Tournilhac, F.; Bosio, L.; Nicoud, J. F.; Simon, J. *Chem. Phys. Lett.* **1988**, *145*, 452. (b) Nguyen, H. T.; Sigaud, G.; Achard, M. F.; Hardouin, F.; Tweig, R. J.; Betterton, K. *Liq. Cryst.* **1991**, *10*, 389. (c) Chiang, Y. H.; Ames, A. E.; Gaudiana, R. H.; Adams, T. G. *Mol. Cryst. Liq. Cryst.* **1991**, *208*, 85. (d) Takenaka, S. *J. Chem. Soc., Chem. Commun.* **1992**, 1748. (e) Pugh, C.; Arehart, S.; Liu, H.; Narayanan, R. *J. Macromol. Sci.—Pure Appl. Chem.* **1994**, *A31*, 1591.

(6) For representative publications on thermotropic liquid crystal phases from semifluorinated alkanes, see: (a) Mahler, W.; Guillon, D.; Skoulios, A. *Mol. Cryst. Liq. Cryst. Lett.* **1985**, *2*, 111. (b) Viney, C.; Twieg, R. J.; Gordon, B. R.; Rabolt, J. F. *Mol. Cryst. Liq. Cryst.* **1991**, *198*, 285. (c) Höpken, J.; Pugh, C.; Richtering, W.; Möller, M. *Makromol. Chem.* **1988**, *189*, 911. (d) Höpken, J.; Faulstich, S.; Möller, M. *Mol. Cryst. Liq. Cryst.* **1992**, *210*, 59.

(7) For selected examples of thermotropic mesophases formed from semifluorinated polymers, see: (a) Wilson, L. M.; Griffin, A. C. *Macromolecules* **1993**, *26*, 6312. (b) Davidson, T.; Griffin, A. C.; Wilson, L. M.; Windle, A. H. *Macromolecules* **1995**, *28*, 354. (c) Jariwala, C. P.; Mathias, L. J. *Macromolecules* **1993**, *26*, 5129. (d) Hoyle, C. E.; Kang, D.; Jariwala, C.; Griffin, A. C. *Polymer* **1993**, *34*, 3070. (e) Wilson, L. M. *Liq. Cryst.* **1994**, *17*, 277. (f) Wilson, L. M.; Griffin, A. C. *Macromolecules* **1994**, *27*, 1928. (g) Wilson, L. M.; Griffin, A. C. *Macromolecules* **1994**, *27*, 4611. (h) Wilson, L. M. *Macromolecules* **1995**, *28*, 325. (i) Wilson, L. M. *Liq. Cryst.* **1995**, *18*, 347.

(8) For selected publications on lyotropic self-assemblies from semifluorinated compounds, see: (a) Turberg, M. P.; Brady, J. E. *J. Am. Chem. Soc.* **1988**, *110*, 7797. (b) Kuwahara, H.; Hamada, M.; Ishikawa, Y.; Kunitake, T. *J. Am. Chem. Soc.* **1993**, *115*, 3002. (c) Giulieri, F.; Krafft, M.-P.; Riess, J. G. *Angew. Chem., Int. Ed. Engl.* **1994**, *33*, 1514.

(9) Percec, V.; Schlueter, D.; Kwon, Y. K.; Blackwell, J.; Möller, M.; Slangen, P. J. *Macromolecules*, in press.

(10) (a) Tamura, M.; Kochi, J. *Synthesis* **1971**, 303. (b) Descoins, C.; Henrick, C. A. *Tetrahedron Lett.* **1972**, 2999.

(11) Demus, D.; Richter, L. *Textures of Liquid Crystals*, Verlag Chemie: Weinheim, 1978.

(12) Coulson, D. R. *Inorg. Synth.* **1972**, *13*, 121.

(13) Moore, J. S.; Stupp, S. I. *Macromolecules* **1990**, *23*, 65.

(14) (a) Gibson, T. *J. Org. Chem.* **1980**, *45*, 1095. (b) Percec, V.; Tomazos, D. *J. Mater. Chem.* **1993**, *3*, 633.

(15) (a) Malthête, J.; Tinh, N. H.; Levelut, A. M. *J. Chem. Soc., Chem. Commun.* **1986**, 1548. (b) Percec, V.; Heck, J. *Polym. Bull.* **1991**, *25*, 431.

(16) Kang, S.-K.; Kim, W.-S.; Moon, B.-H. *Synthesis* **1985**, 1161.

(17) Ames, D. E.; Islip, P. J. *J. Chem. Soc.* **1963**, 4363.

(18) Bernady, K. F.; Floyd, M. B.; Poletto, J. F.; Weiss, M. J. *J. Org. Chem.* **1979**, *44*, 1438.

(19) Buendia, J. *Bull. Soc. Chim. Fr.* **1966**, 2778.

(20) (a) Ishihara, T.; Kuroboshi, M.; Okada, Y. *Chem. Lett.* **1986**, 1895. (b) Chen, Q.-Y.; Yang, Z. Y.; Zhao, C.-X.; Qiu, Z.-M. *J. Chem. Soc., Perkin Trans. 1*, **1988**, 563.

(21) Nystrom, R. F.; Brown, W. G. *J. Org. Chem.* **1947**, *10*, 1197.

(22) Dakka, G.; Sasson, Y. *Tetrahedron Lett.* **1987**, *28*, 1223.

(23) Höpken, J.; Möller, M.; Boileau, S. *New Polym. Mater.* **1991**, *2*, 339.

(24) (a) Kraus, G. A.; Landgrebe, K. *Synthesis* **1984**, 885. (b) Percec, V.; Hsu, C. S.; Tomazos, D. *J. Polym. Sci.: Part A: Polym. Chem. Ed.* **1988**, *26*, 2047.

(25) Lyle, R. E.; DeWitt, E. J.; Pattison, I. C. *J. Org. Chem.* **1956**, *21*, 61.

(26) Neumann, W. P. *Synthesis* **1987**, 665.

(27) Boss, R.; Scheffold, R. *Angew. Chem., Int. Ed. Engl.* **1976**, *15*, 558.

(28) Yang, Z.-Y.; Burton, D. J. *Tetrahedron Lett.* **1991**, *32*, 1019.

(29) (a) Girard, P.; Namy, J. L.; Kagan, H. B. *J. Am. Chem. Soc.* **1980**, *102*, 2693. (b) Inanaga, J.; Ishikawa, M.; Yamaguchi, M. *Chem. Lett.* **1987**, 1485.

(30) Dunlap, R. D.; Bedford, R. G.; Woodbrey, J. C.; Furrow, S. D. *J. Am. Chem. Soc.* **1959**, *81*, 2927.

(31) (a) Percec, V.; Keller, A. *Macromolecules* **1990**, *23*, 4347. (b) Keller, A.; Ungar, G.; Percec, V. In *Advances in Liquid Crystalline Polymers*; Weiss, R. A., Ober, C. K., Eds.; ACS Symposium Series 435, American Chemical Society: Washington, DC, 1990; p 308.

(32) For a recent review on self-assembly *via* tapered groups, see: Percec, V.; Johansson, G. In *Macromolecular Design of Polymeric Materials*; Hatada, K., Katayama, T., Vögl, O., Eds.; Dekker: New York, in press.

(33) For recent examples of self-assembly of new supramolecular architectures *via* tapered groups, see, for example: (a) Serrete, A. G.; Swager, T. M. *J. Am. Chem. Soc.* **1993**, *115*, 8879. (b) Serrette, A. G.; Swager, T. M. *Angew. Chem., Int. Ed. Engl.* **1994**, *33*, 2342. (c) Zheng, H.; Swager, T. M. *J. Am. Chem. Soc.* **1994**, *116*, 761. (d) Xu, B.; Swager, T. M. *J. Am. Chem. Soc.* **1995**, *117*, 5011.

MA9511558